Magnetic-field-induced localization in narrow-gap semiconductors $Hg_{1-x}Cd_xTe$ and InSb

M. Shayegan and V. J. Goldman
Department of Electrical Engineering, Princeton University, Princeton, New Jersey 08544

H. D. Drew
Department of Physics and Astronomy, University of Maryland, College Park, Maryland 20742
(Received 16 February 1988)

Magnetotransport measurements on *n*-type $Hg_{1-x}Cd_xTe$ ($x \simeq 0.2$) and InSb and far-infrared magnetooptical spectroscopy in $Hg_{1-x}Cd_xTe$ are reported. The transport data at magnetic fields below and near the magnetic-field-induced metal-insulator (*M-I*) transition indicate clear similarity of $Hg_{1-x}Cd_xTe$ and InSb. At fields well above the *M-I* transition and at low temperatures, the magnetotransport coefficients for $Hg_{1-x}Cd_xTe$ show anomalously weak dependences on field and temperature. This is attributed to shorting of the bulk by a conducting surface layer. Below the *M-I* transition field, an anomalous Hall effect is observed in both $Hg_{1-x}Cd_xTe$ and InSb. We interpret this effect within a model in which the *M-I* transition takes place in the donor impurity band. The impurity cyclotron resonance observed in $Hg_{1-x}Cd_xTe$ provides conclusive evidence for donor-bound electrons in this semiconductor and further confirms its similarity to InSb. The cyclotron-resonance data are in agreement with theoretical predictions for hydrogenic donors in a strong magnetic field. These observations provide strong evidence against the Wigner crystallization of electrons in $Hg_{1-x}Cd_xTe$.

I. INTRODUCTION

Consider a moderately doped (*n*-type) semiconductor, which exhibits metallic behavior at low temperatures, subjected to an intense magnetic field. In the extreme quantum magnetic limit, where only the lowest spin-polarized Landau level is occupied, the electron Fermi energy E_F (measured relative to the bottom of the lowest Landau level) decreases as $1/B^2$ so that the ratio of the electron Coulomb energy E_C ($\sim e^2 n^{1/3}$) to the kinetic energy E_K ($E_K \sim E_F$) can become very large (B is the magnetic field strength and n is the electron density). When E_C/E_K is large, and if the ionized impurities that generate the carriers are considered to be a uniformly charged (jellium) background and the effects of disorder are neglected so that the system can be idealized as a free-electron system, then various highly correlated electron states such as a charge-density wave or a Wigner crystal may ensue.[1] On the other hand, in a uniformly doped semiconductor, the interaction between electrons and the randomly distributed ionized impurities is always present. This interaction, which is at least as strong as the electron-electron interaction, can (and usually does) lead to a ground state in which the electrons are bound on impurities and the so-called magnetic freeze-out effect is observed.[2-6]

The magnetic-field-induced metal-insulator (*M-I*) transition in narrow-gap semiconductors such as InSb and $Hg_{1-x}Cd_xTe$ ($x \simeq 0.2$) has been the subject of much interest. Although some of the early results on InSb were interpreted in terms of Wigner condensation of electrons,[7] it is well established by now that the magnetic freeze-out effect takes place in this material.[2-6] The case of $Hg_{1-x}Cd_xTe$, however, has remained controversial. Several years ago, Nimtz *et al.*[8] interpreted an anomalously weak magnetoresistance observed in $Hg_{1-x}Cd_xTe$ at high magnetic fields as evidence for an electronic phase transition into a Wigner crystal. Magnetotransport studies by several groups that followed were often not consistent with each other and led to much controversy. The results were interpreted as evidence for magnetic freeze-out,[9,10] Anderson localization,[11,12] Mott transition,[13] and Wigner crystallization.[14-17] This latter interpretation is especially surprising, however, in view of the similarity of the electronic structure of $Hg_{1-x}Cd_xTe$ to InSb.

In this paper we present the results of our extensive study of the magnetotransport and far-infrared magnetooptical properties of well-characterized samples of state of the art $Hg_{1-x}Cd_xTe$ at low temperatures and high magnetic fields.[18-24] The results establish the following. (1) The transport data of $Hg_{1-x}Cd_xTe$ are indeed very similar to those of InSb at magnetic fields near and below the *M-I* transition. Only at fields well above the *M-I* transition anomalous features are observed for $Hg_{1-x}Cd_xTe$. These anomalies can be attributed to the shorting of the bulk by a conducting surface layer. This observation casts doubt on the Wigner-crystal interpretation which has been based on such anomalous features.[8,17] Below the *M-I* transition field in *both* $Hg_{1-x}Cd_xTe$ and InSb we observe an anomalous Hall effect. This anomaly can be interpreted within a model in which the *M-I* transition in InSb and $Hg_{1-x}Cd_xTe$ takes place in the donor impurity band. (2) Conclusive and direct spectroscopic evidence that at high magnetic fields the electrons are indeed bound on shallow donors in the ground state is provided by the magnetooptical transitions in $Hg_{1-x}Cd_xTe$. We report far-infrared transmission experiments which indicate the presence of impurity cyclotron resonance in $Hg_{1-x}Cd_xTe$ at low temperatures

 ©1988 The American Physical Society

and at magnetic fields above and near the *M-I* transition. The magnitude of the absorption shows that (within the experimental accuracy) nearly all the electrons are bound on shallow donors. Our magnetotransport and cyclotron-resonance data therefore establish that the magnetic-field-induced *M-I* transition in $Hg_{1-x}Cd_xTe$ occurs in the impurity band and is not a manifestation of Wigner crystallization of electrons.

In Sec. II we present some general considerations regarding the *M-I* transition in crystalline semiconductors doped with shallow impurities. In Secs. III and IV we present and discuss the magnetotransport and magnetooptical results, respectively. Finally, we summarize our conclusions in Sec. V.

II. GENERAL CONSIDERATIONS

Although the metal-insulator (*M-I*) transition in doped semiconductors has been studied for many years,[25,26] our understanding of this phenomenon is far from complete. Early contributions by Mott and Anderson emphasized the importance of electron correlations and disorder, respectively. The concepts of a mobility edge and smooth potential fluctuations have proved to be fruitful in the pictures of the *M-I* transition in amorphous semiconductors and two-dimensional electron systems.[27] The nature of the disorder, however, is different in crystalline semiconductors doped with shallow (hydrogenic) impurities. At high impurity concentrations, such that $a^* n^{1/3} \gg 1$, where n is the electron concentration and a^* is the effective donor Bohr radius, the interaction energy between the conduction-band electrons and the ionized impurities E_i is of the order $e^2 n^{1/3}/\kappa$, where κ is the static dielectric constant of the crystal. On the other hand, the Fermi energy is $E_F \sim \hbar^2 n^{2/3}/m^*$, where m^* is the conduction-band effective mass. Therefore, at such impurity concentrations $E_i/E_F \sim (a^* n^{1/3})^{-1} \ll 1$, and the electrons can be treated as a nearly ideal gas.[28] Closer to the *M-I* transition, however, the screening is not effective and the electron-impurity interaction is strong for small separations and cannot be well approximated by a smooth effective potential. In addition, the origin of the disorder in crystalline semiconductors lies chiefly in the randomness of the spacial distribution of shallow impurities and not in the difference in the strengths of the interaction or spacial fluctuations in the band-edge energy. It is well established that at sufficiently low impurity concentrations the so-called impurity band is formed;[25] however, there is no general agreement on whether the *M-I* transition takes place in the impurity band alone or whether the hybridized conduction-band states play an important role.[27]

Although not widely known, there exist several pieces of direct evidence that the *M-I* transition occurs in the impurity band. Indeed, infrared transmission experiments performed in narrow-band-gap semiconductor InSb,[5] and also recently on GaAs,[29] revealed that the absorption due to electronic transitions between donor-bound states persists at magnetic fields well below the magnetic-field-induced *M-I* transition. The magnitude of the absorption implies that nearly all donor-band electrons participate in the optical transitions at low temperatures. In another experiment, cyclotron resonance of conduction-band electrons was observed in wide-band-gap insulating CdSe at helium temperatures under thermal equilibrium conditions.[30] The origin of the implied extended electronic states was attributed to the *M-I* transition in small clusters of donors of higher than average concentration, resulting from random fluctuations of local donor density.

These experimental results support the tight-binding approach to the donor band in the vicinity of the *M-I* transition. Our observed magnetotransport and magnetooptical data on $Hg_{1-x}Cd_xTe$ and InSb reported in this paper are consistent with this view. We present a model based on a tight-binding picture for the donor electrons and a random spacial distribution of donors.[22] We apply this model to the anomalous Hall effect near, but below the magnetic-field-induced *M-I* transition in both InSb and $Hg_{1-x}Cd_xTe$. According to this model, below the *M-I* transition, the semiconductor crystal contains an infinite metallic donor cluster as well as shallow donors which do not have close neighbors and thus give rise to effectively localized electronic states. Additional evidence for this assumption is provided by the observation of impurity cyclotron resonance below the *M-I* transition field. The results, therefore, establish that the magnetic-field-induced *M-I* transition in these narrow-band-gap semiconductors takes place in the donor impurity band.

III. MAGNETOTRANSPORT COEFFICIENTS

In the following sections we present the transport measurements made on samples of n-type $Hg_{1-x}Cd_xTe$ ($x \simeq 0.2$) in wide ranges of carrier density ($1.1\times10^{14} \lesssim n \lesssim 1.8\times10^{15}$ cm^{-3}), magnetic field (up to 19 T), and temperature ($0.08 < T < 77$ K). Also presented are data on two samples of n-type InSb. Section III A describes the experimental details. In Sec. III B general features of the magnetotransport data in different ranges of magnetic field are presented, while a more detailed discussion of the data is given in Sec. III C. In Sec. III D we review some of the anomalous features in the transport data of $Hg_{1-x}Cd_xTe$ which have been interpreted in the past as evidence for Wigner crystallization of electrons in this material. We show how these anomalies can be understood as experimental artifacts. Finally, we summarize our conclusions based on the magnetotransport data in Sec. III E.

A. Experimental details

Magnetotransport measurements were made on n-type, bulk, narrow-band-gap semiconductors $Hg_{1-x}Cd_xTe$ with $x \sim 0.2$ (band gap $E_g \simeq 0.1$ eV, effective mass $m^* \simeq 0.007 m_e$, dielectric constant $\kappa \simeq 17$) and InSb ($E_g = 0.24$ eV, $m^* = 0.014 m_e$, $\kappa = 16$). The relevant parameters for these samples are listed in Table I. The electron densities and mobilities listed are from low-field measurements at 77 K. The $Hg_{1-x}Cd_xTe$ samples were grown at Honeywell. Characterization of these samples in terms of their purity, crystallinity, and compositional uniformity (typical variations in x are ± 0.002) (Ref. 31)

TABLE I. Important parameters of the samples studied. Samples denoted by capital letters are $Hg_{1-x}Cd_xTe$ with the indicated x.

Sample	x	n (77 K) (10^{14} cm^{-3})	μ (77 K) (10^5 cm^2/V s)	B_0 (T)	$B_{M\text{-}I}$ (T)
A	0.208	2.5	2.5	0.22	
B	0.208	12	1.8	0.55	3.6
C	0.208	7.2	1.9	0.41	2.6
D	0.208	1.1	1.9	0.12	0.5
H	0.204	0.3	2.7		
I	0.184	1.4	4.5		
J	0.208	1.1	2.6		0.5
K	0.208	2.7	2.8	0.22	1.1
L	0.208	7.0	1.9	0.39	2.3
M	0.208	4.8	2.1	0.29	1.6
P	0.212	5.4	2.0	0.35	2.0
Q	0.199	18	2.2	0.74	6.0
Y	0.224	0.6	1.2		
InSb-1		22	2.4	0.81	3.3
InSb-2		55	1.9	1.5	5.8

indicates that they are state of the art bulk $Hg_{1-x}Cd_xTe$. Comparing the mobility values with calculations,[32] we estimate the compensation (the ratio of the number of acceptors to donors) to be fairly small (typically $\lesssim 0.3$) in these samples. The InSb samples were obtained from Cominco. These are also high-quality samples with compensation $\lesssim 0.1$.

The preparation of samples for transport measurements was a crucial step in these experiments. It is well known by now that the transport properties of $Hg_{1-x}Cd_xTe$ can be significantly influenced by a conducting surface layer that eventually shorts out the bulk once the bulk resistance becomes sufficiently large.[15,19,20,33–35] The exact nature and origin of this surface layer are not known yet; however, it is probably related to the preferential out-diffusion of Hg near the surface (leaving behind a Te-rich compound) and/or to the presence of oxides and damage near the surface.[33,35–37] We learned in our experiments that although most of the surface layer can be removed by etching, the surface degrades in a short time when exposed to air at room temperature. Our observation is in qualitative agreement with the results of recent work by Balev *et al.*,[35] who measured the magnetotransport coefficients of n-type $Hg_{1-x}Cd_xTe$ as a function of the time elapsed after etching the samples. In the studies reported here, we tried to keep the time between the etching and cooling the samples in liquid nitrogen as short as possible. However, we were not able to eliminate the surface problem entirely.

The $Hg_{1-x}Cd_xTe$ samples were cleaved into rectangular plates (typical dimensions $\sim 2\times 7\times 0.5$ mm^3). A string saw was used to cut the InSb samples into similar shape and dimensions. The samples were then etched in a bromine (3%)–methanol (97%) solution, and electrical leads were soldered to them with indium. In soldering the leads, care was exercised so that only sufficient heat to melt the indium at the contact was applied. For measurements in the temperature range $0.4 \lesssim T \lesssim 4.2$ K, samples were immersed in ^{3}He or ^{4}He baths and the temperature was controlled by pumping on the bath and using the He vapor pressure to monitor the temperature. Above 4.2 K, a variable-temperature cryostat was employed and a calibrated carbon-glass resistor was used as a thermometer. A dilution refrigerator was used for measurements below 0.4 K.[20] The accuracy in our reported temperatures is estimated to be about 3%.

All the transport measurements were made in Bitter magnets at the Francis Bitter National Magnet Laboratory at the Massachusetts Institute of Technology (MIT). We measured the longitudinal (ρ_{zz}), transverse (ρ_{xx}), and Hall (ρ_{xy}) resistivities. Denoting the direction of the magnetic field by $\hat{z}$, ρ_{zz} refers to the resistivity along $\hat{z}$, ρ_{xx} to the resistivity along x, and ρ_{xy} to the conventional Hall resistivity (the current direction is along $\hat{z}$ for ρ_{zz} and along $\hat{x}$ for ρ_{xx} and ρ_{xy}). All the measurements were made using the dc technique. The data acquisition and subsequent analysis were done using a computer. Because of the imperfect positions of the contacts, it was usually necessary to correct the data to eliminate the contribution of ρ_{xx} to ρ_{xy} and vice versa. In *all* of our reported data, ρ_{xx} and ρ_{xy} were measured for opposite directions of the magnetic field and the data were added (subtracted) to obtain ρ_{xx} (ρ_{xy}). The corrections are especially important when measuring ρ_{xy} at high magnetic fields and low temperatures where ρ_{xx} is very large and can dramatically influence ρ_{xy} if the corrections are not made.

B. Magnetotransport results

In Figs. 1–3 we show log-log plots of ρ_{zz}, ρ_{xx}, and ρ_{xy} versus magnetic field B for an InSb sample and two $Hg_{1-x}Cd_xTe$ samples (K and B) at low temperatures. These figures give an overall view of the magnetotransport data in these materials. The important features of the data are the following. (1) In the absence of magnetic

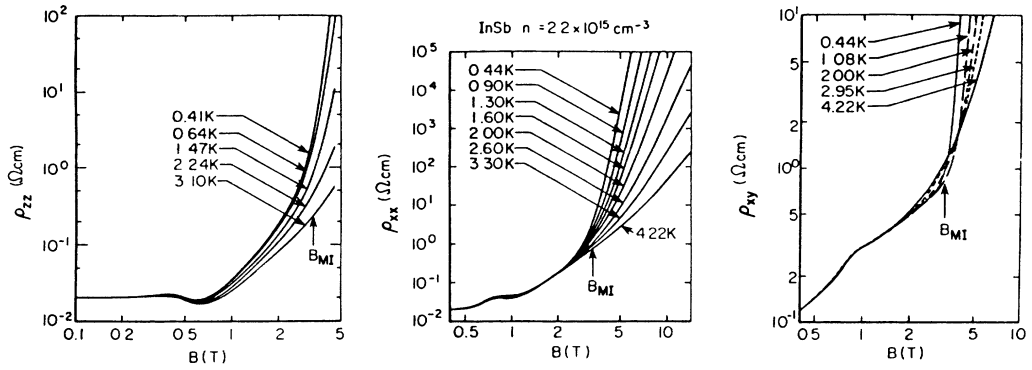

FIG. 1. Longitudinal (ρ_{zz}), transverse (ρ_{xx}), and Hall (ρ_{xy}) resistivities of an n-type InSb sample shown for the indicated temperatures as a function of the magnetic field B. At low temperatures, above the metal-insulator transition field $B_{M\text{-}I}$ all the resistivities rapidly increase with increasing B.

field the transport coefficients for all of the samples listed in Table I are weakly temperature dependent (metallic behavior). (2) As B is increased, the transport data show stronger temperature dependences. We denote the magnetic field above which ρ_{xy} abruptly rises at low temperatures as the M-I transition field $B_{M\text{-}I}$ (see Figs. 1–3). Note that ρ_{zz} and ρ_{xx} also show a strong magnetoresistance above $B_{M\text{-}I}$. (3) At magnetic fields well above $B_{M\text{-}I}$, the $Hg_{1-x}Cd_xTe$ data show a much weaker dependence on temperature and magnetic field than what is expected for the magnetic freeze-out effect and is observed for InSb (see Figs. 1–3). (4) Below $B_{M\text{-}I}$ the data for $Hg_{1-x}Cd_xTe$ and InSb are very similar. At low temperatures, ρ_{xy} data show an anomalous "Hall dip," i.e., the Hall coefficient $R_H \equiv \rho_{xy}/B$ falls below its low-field value. We now present the data in more detail.

In Figs. 4 and 5, ρ_{zz}, ρ_{xx}, and ρ_{xy} for two InSb and two $Hg_{0.79}Cd_{0.21}Te$ samples (K and B) are shown in the low-field range where the Shubnikov–de Haas (SdH) oscillations are observed. The data for the two semiconductors are similar both qualitatively and quantatively. For instance, the last SdH maximum in ρ_{xx} is expected to occur at a magnetic field B_0 approximately given by[38]

$$B_0 = (\pi^2/\sqrt{2})^{2/3}(2\hbar/e)n^{2/3} . \quad (1)$$

This expression is valid at low temperatures ($k_B T \ll \hbar\omega_c$) and for low effective mass ($m^*/m_e \ll 1$), where $\omega_c = eB/m^*$ is the cyclotron frequency. The measured B_0 for the samples we studied are listed in Table I and are plotted versus density n (as measured from the Hall data) in Fig. 6. We also plot the dependence of B_0

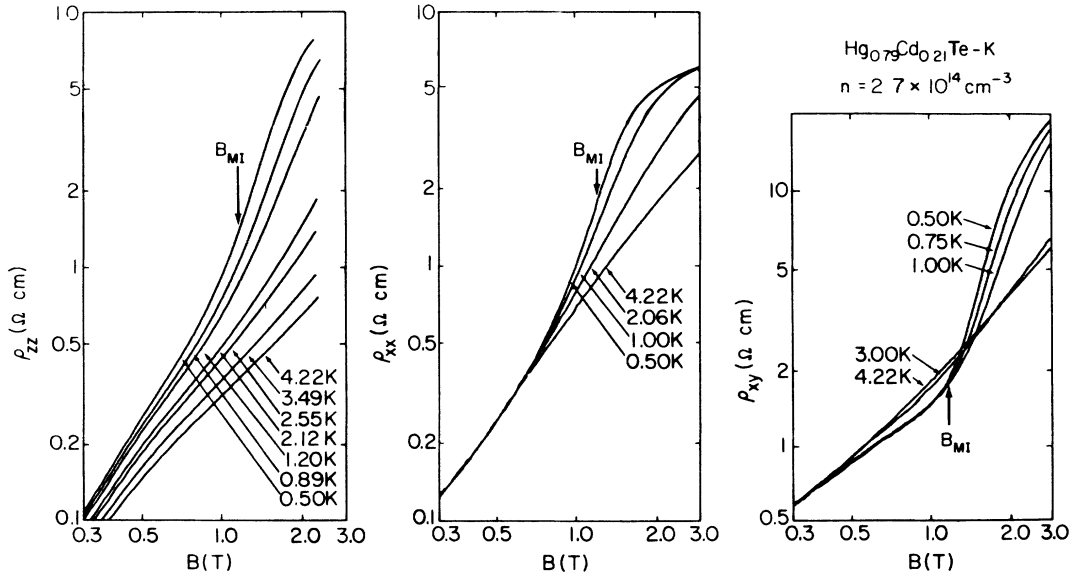

FIG. 2. ρ_{zz}, ρ_{xx}, and ρ_{xy} data shown for an n-type $Hg_{0.79}Cd_{0.21}Te$ sample (sample K in Table I). In the field range $B < B_{M\text{-}I}$, the resistivities show behavior similar to the InSb data of Fig. 1. Above $B_{M\text{-}I}$, however, the relatively weak field and temperature dependencies of the resistivities at low temperatures observed in this figure are in contrast to the InSb data.

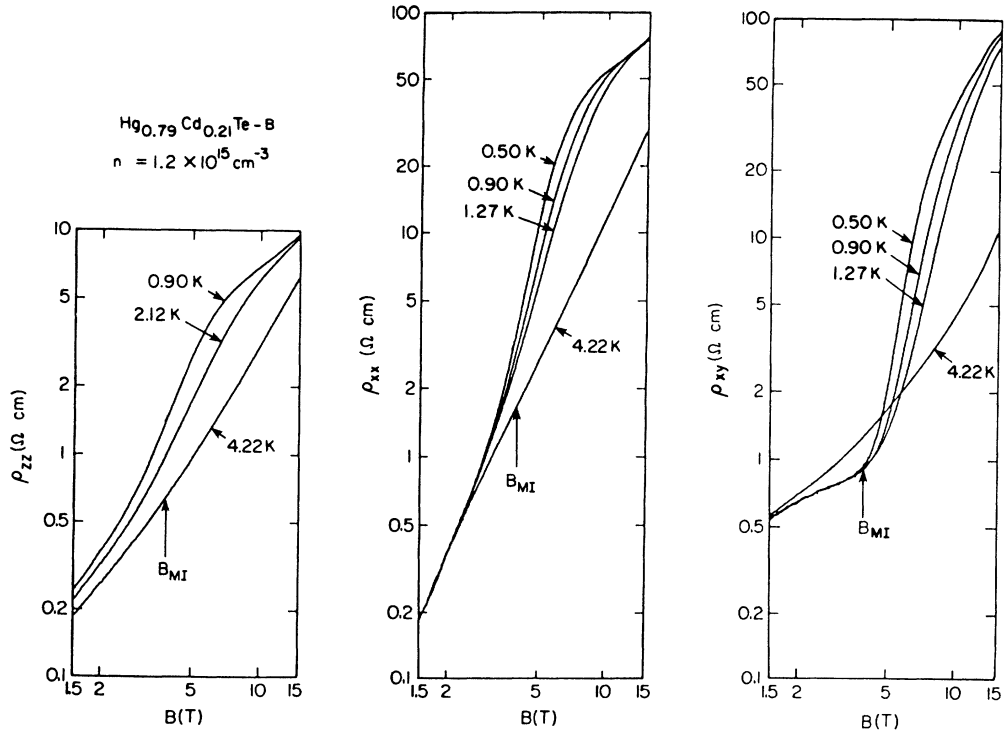

FIG. 3. ρ_{zz}, ρ_{xx}, and ρ_{xy} data shown for another $Hg_{0.79}Cd_{0.21}Te$ sample with a higher carrier density (B in Table I). These data are similar to those in Fig. 2 and are in contrast to the InSb data (at fields $B > B_{M\text{-}I}$) of Fig. 1.

on n as given by Eq. (1) (dashed line in Fig. 6). The very good agreement between the predicted and observed positions of the last SdH maximum seen in Fig. 6 is impressive, especially since there are no adjustable parameters for either semiconductor. It is also worth noting that the agreement between B_0 in Eq. (1) and the observed value extends to higher densities [$B_0 = 5.4$ T both experimentally[39] and according to Eq. (1) for $Hg_{0.82}Cd_{0.18}Te$ with $n = 3.8 \times 10^{16}$ cm^{-3}].

Previously, an anomalous peak in ρ_{xx} above the last SdH maximum was reported[40] and was claimed to be the evidence for a resonant state above the conduction-band minimum in $Hg_{1-x}Cd_xTe$. This anomalous peak was reported to shift to lower magnetic fields as a function of increasing carrier density.[40] From our studies, two conclusions can be clearly made. First, for the samples we studied, no such anomalous feature was observed. Second, our observed B_0 for both $Hg_{1-x}Cd_xTe$ and InSb agree with the expected values quite well.

In Figs. 1–3 the data indicate that as B is sufficiently

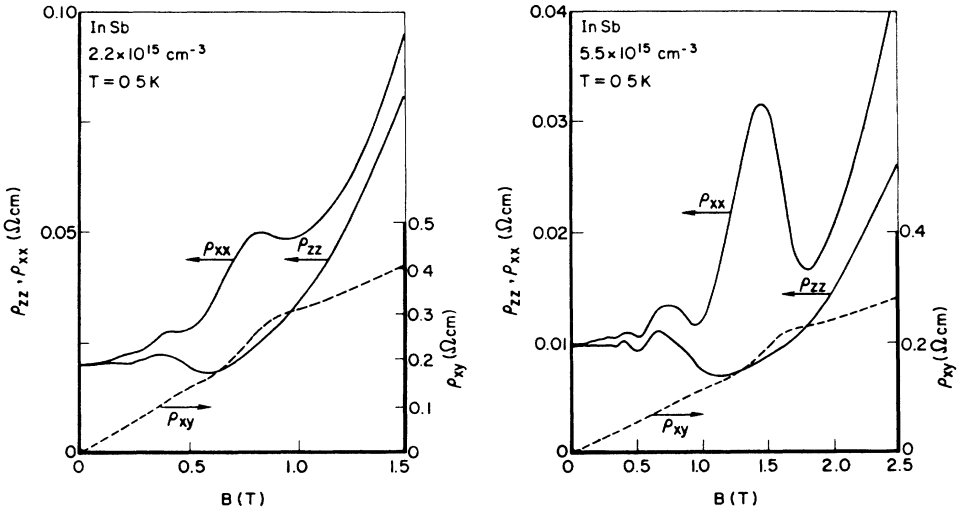

FIG. 4. ρ_{zz}, ρ_{xx}, and ρ_{xy} data for two InSb samples with different carrier densities are shown in the low-field range where the Shubnikov—de Haas quantum oscillations are observed.

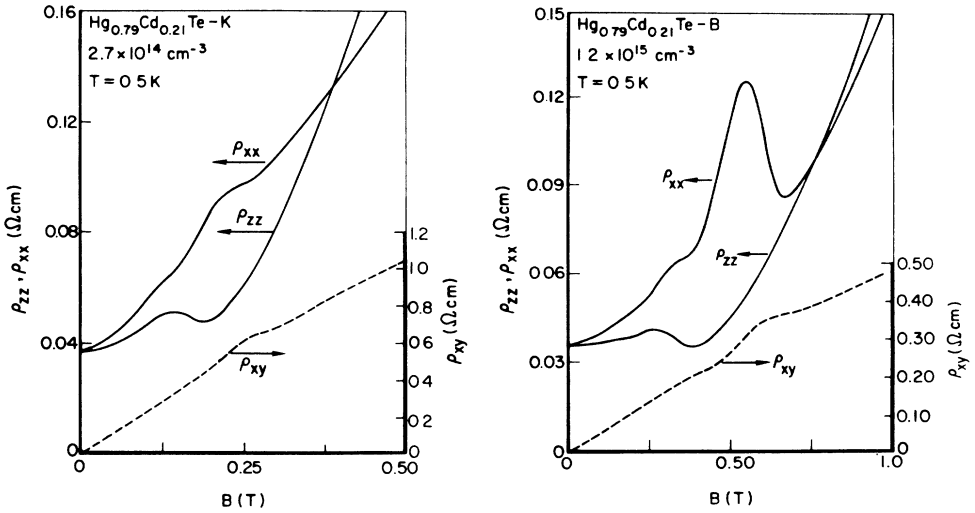

FIG. 5. ρ_{zz}, ρ_{xx}, and ρ_{xy} data shown for two $Hg_{0.79}Cd_{0.21}Te$ samples (K and B) in the low-field range. The data are qualitatively and quantitatively similar to the InSb data in Fig. 4.

increased ρ_{xy} abruptly rises. We define the magnetic field at which ρ_{xy} abruptly rises as the M-I transition field $B_{M\text{-}I}$. Above $B_{M\text{-}I}$, all three resistivities ρ_{zz}, ρ_{xx}, and ρ_{xy} increase strongly with increasing field or decreasing temperature for InSb (Fig. 1). For $Hg_{1-x}Cd_xTe$, however, no such strong dependence on temperature or field is observed for magnetic fields well above $B_{M\text{-}I}$. In Figs. 1–3 it is evident that the rise in ρ_{xy} becomes less sharp at higher temperatures and, therefore, a precise definition of

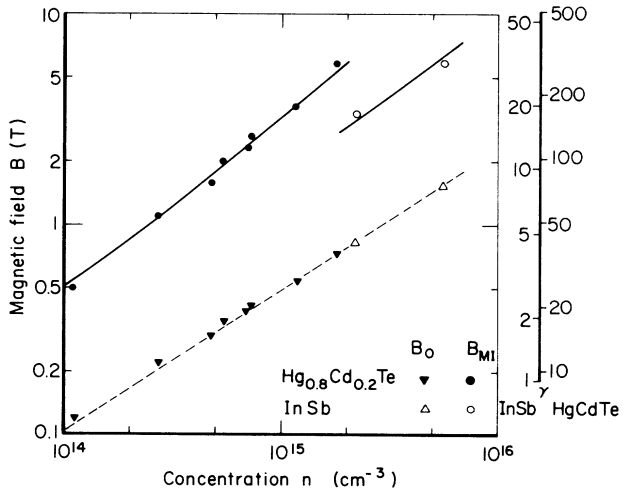

FIG. 6. Observed metal-insulator transition fields $B_{M\text{-}I}$ (circles) and the positions of the last maximum in the Shubnikov–de Haas oscillations B_0 (triangles) plotted vs the carrier density for the $Hg_{0.8}Cd_{0.2}Te$ and InSb samples. The dashed line is the predicted B_0 based on Eq. (1). The solid curves represent the metal-insulator transition field vs density calculated using Eq. (3) with $\delta=0.31$ (0.34) for $Hg_{0.8}Cd_{0.2}Te$ (InSb), respectively (see text). On the right, the parameter γ in Eq. (2) is indicated for the two semiconductors as a function of the magnetic field.

$B_{M\text{-}I}$ at finite temperatures is difficult. A discussion of $B_{M\text{-}I}$, including its dependence on carrier density and its relation to the other transport coefficients, will be given in Sec. III C.

The dependence of ρ_{xy} on B in the magnetic field range below $B_{M\text{-}I}$ is anomalous (Figs. 1–3). At low temperatures, the Hall coefficient $R_H(B)=\rho_{xy}(B)/B$ displays a "Hall dip."[18,19,22] In Figs. 7 and 8 the ρ_{xy}-versus-B data near and below $B_{M\text{-}I}$ for several $Hg_{1-x}Cd_xTe$ and InSb samples are shown. Note that as the temperature is increased, this dip gradually disappears and the Hall resistivity rises to a high-temperature value consistent with the low-field carrier concentration. We discuss the interpretation of this anomalous Hall dip in Sec. III C.

As mentioned before, the $Hg_{1-x}Cd_xTe$ transport data in the field range well above $B_{M\text{-}I}$ and at low temperatures are anomalous. In Fig. 1 we observe that, for InSb, the resistivities increase by several orders of magnitude (relative to the low-field values) in the high-field range above $B_{M\text{-}I}$. In the case of $Hg_{1-x}Cd_xTe$ (Figs. 2 and 3), however, the temperature and field dependencies are much weaker than those observed for InSb. This diverging behavior at high fields is especially surprising because in this field range it is expected that the electron's Coulomb interaction with the ionized impurities dominates, resulting in the magnetic freeze-out of carriers as observed in InSb. Nevertheless, this anomalous feature led Nimtz *et al.*[8,14] and recently Rosenbaum *et al.*[17] to believe that an electronic phase transition into a Wigner crystal takes place in $Hg_{1-x}Cd_xTe$.

We studied the magnetotransport coefficients of several $Hg_{1-x}Cd_xTe$ samples at high fields and low temperatures. The results can be summarized as follows. (1) In *all* cases the weak field dependence at low temperatures was observed. For instance, in Fig. 9 ρ_{xx} data are shown for three samples with different carrier densities. For all these samples, a distinctly weak dependence of ρ_{xx} on B for fields above $B_{M\text{-}I}$ is observed at $T=0.5$ K. (2) We ob-

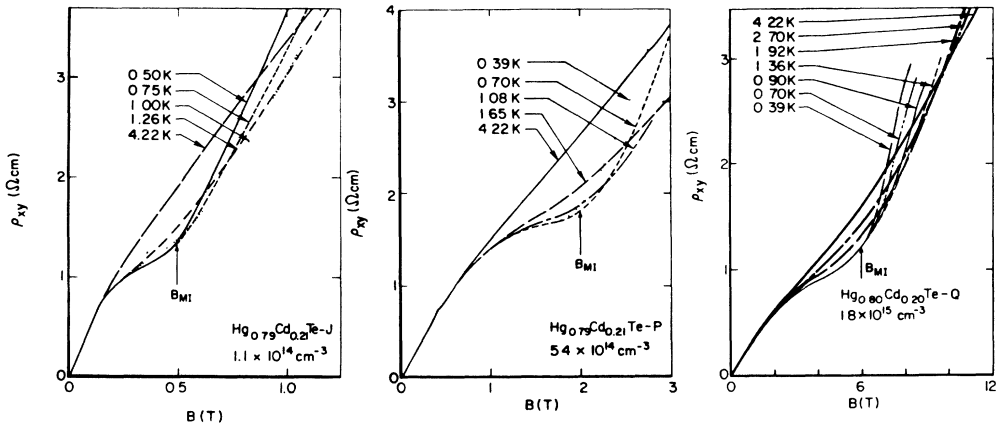

FIG. 7. Hall resistivity ρ_{xy} shown for three $Hg_{0.8}Cd_{0.2}Te$ samples (J, P, and Q in Table I). Similar to the data shown in Figs. 1–3 and 8, the ρ_{xy} display "Hall dips" in the field range below the metal-insulator transition fields $B_{M\text{-}I}$ and at low temperatures.

served that the onset of this weak dependence (at a fixed low temperature, e.g., 0.5 K) depends on sample preparation. In specific, the onset shifts to higher magnetic fields for samples that are freshly etched and quickly mounted in the cryostat. This observation is in agreement with the results recently reported by Balev *et al.*,[35] who made measurements of the transport coefficients in $Hg_{1-x}Cd_xTe$ as a function of time after etching. (3) In a few cases, we observed SdH oscillations in resistivities at magnetic fields well above $B_{M\text{-}I}$. An example is shown in Fig. 10 [solid curve labeled (a)]. The frequency of these oscillations suggests a density $\sim 10^{18}$ cm^{-3}, well above the carrier density for this sample. Suspecting that the oscillations are due to a high-mobility surface layer, we removed the sample from the cryostat and bombarded its surface using a sand-blaster with fine-size beads. We then remounted the sample in the cryostat and remeasured the magnetoresistance. The remeasured ρ_{xx} data are also shown in Fig. 10 [curves labeled (b)]. Note the disappearance of the high-field SdH oscillations.

In Fig. 11 the temperature dependence of ρ_{zz} for two $Hg_{1-x}Cd_xTe$ samples are shown. Note that at low temperatures and high magnetic fields the data are essentially temperature independent. For comparison, similar data are shown in Fig. 12 for an InSb sample. Note that for InSb a strong temperature dependence is observed down to the lowest experimental temperatures. At low temperatures ($T \lesssim 1.5$ K) and for magnetic fields above $B_{M\text{-}I}$ the InSb data show a $\ln(\rho_{zz}) \sim T^{-m}$ behavior with $m \simeq 0.3$. This observation is consistent with previously reported

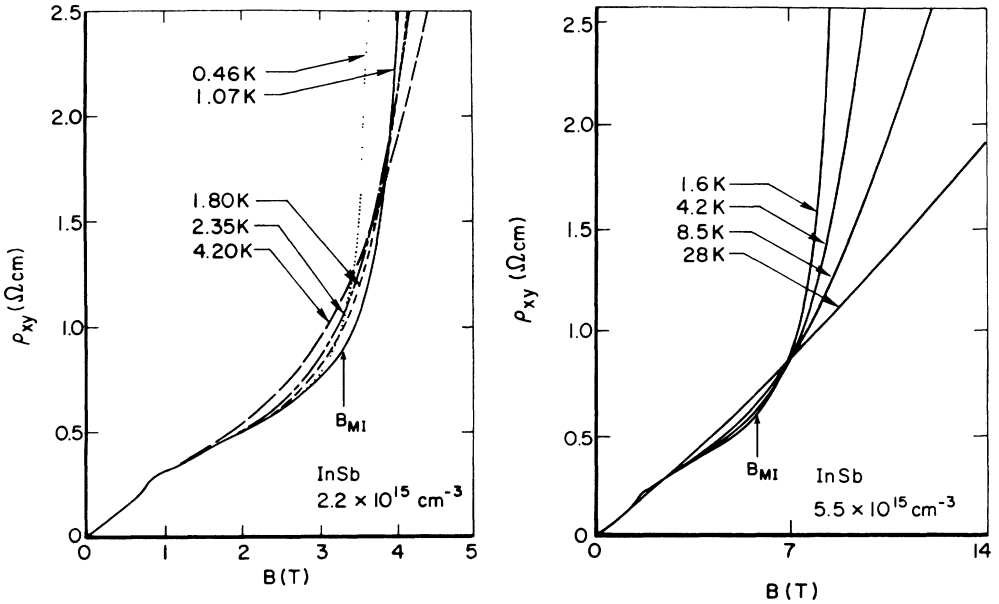

FIG. 8. ρ_{xy} data plotted for two InSb samples showing "Hall dips" similar to the $Hg_{08}Cd_{0.2}Te$ data (Figs. 2, 3, and 7) at low temperatures. At higher temperatures, the Hall dip gradually disappears and ρ_{xy} rises to a high-temperature value consistent with the low-field carrier concentration.

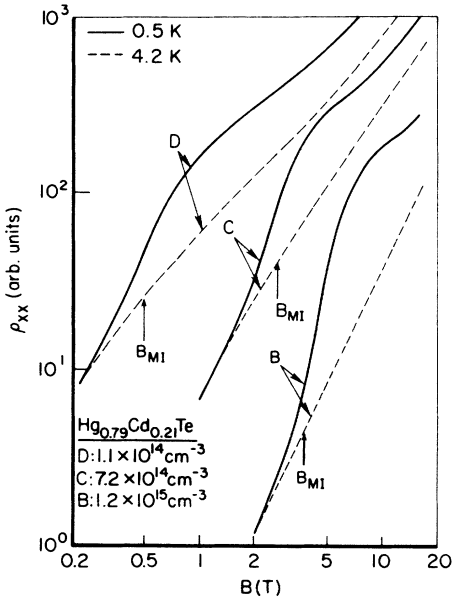

FIG. 9. ρ_{xx} data shown for three $Hg_{0.79}Cd_{0.21}Te$ samples (B, C, and D), showing the anomalously weak magnetoresistance above the metal-insulator transition $B_{M\text{-}I}$ at low temperatures. This effect is attributed to the shorting of the bulk by a conducting surface layer (see text).

results on InSb (fourth paper in Ref. 3), where the temperature dependencies were interpreted in terms of variable-range-hopping conduction models.

Based on these observations, and in agreement with conclusions of previous work,[15,19,20,33,35] we believe that the anomalously weak magnetoresistivity in $Hg_{1-x}Cd_xTe$ at low temperatures and high fields is due to a conducting surface layer that eventually shorts out the bulk when the bulk resistance becomes sufficiently large.

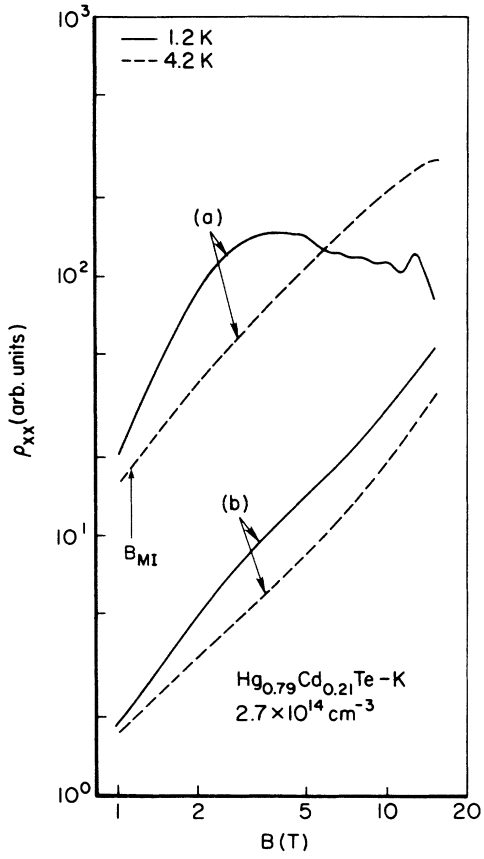

FIG. 10. ρ_{xx} data shown for a $Hg_{0.79}Cd_{0.21}Te$ sample (K). In (a) oscillations in ρ_{xx} are observed at low temperature and at magnetic fields well above $B_{M\text{-}I}$. These are attributed to a high-mobility surface layer. In (b) the remeasured data for the same sample are shown after the surface was roughened (see text) to reduce the mobility of the surface layer. The disappearance of the oscillations confirms the reduction of the surface conductivity.

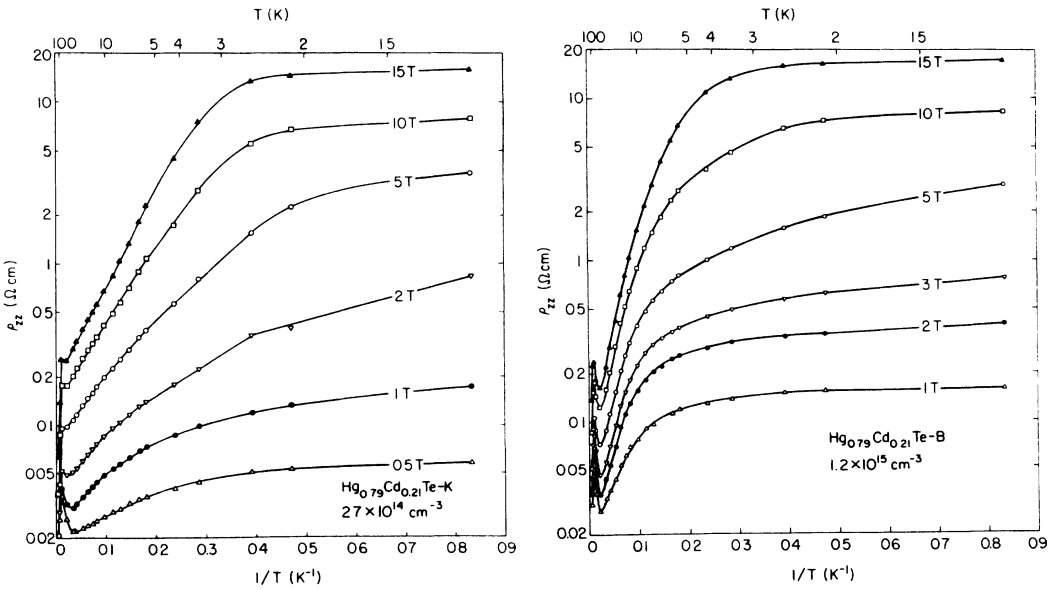

FIG. 11. Plots of $\log_{10}\rho_{zz}$ vs $1/T$ are shown for two $Hg_{0.79}Cd_{0.21}Te$ samples (K and B). The weak temperature dependence of ρ_{zz} at high magnetic fields above $B_{M\text{-}I}$ and at low temperatures is in contrast to the InSb data (Fig. 12) and is attributed to the conducting surface layer.

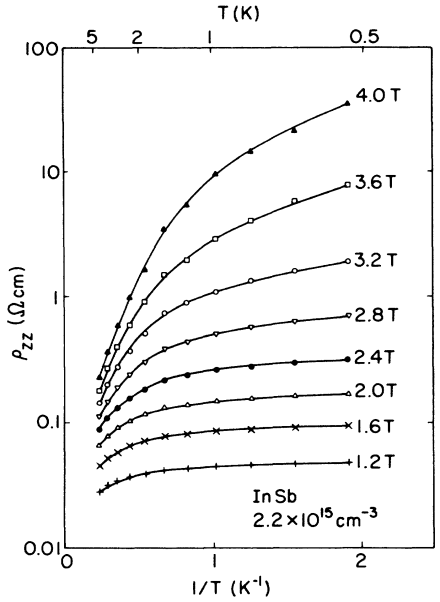

FIG. 12. Plots of $\log_{10}\rho_{zz}$ vs $1/T$ are shown for InSb. The strong dependence of ρ_{zz} on temperature down to the lowest temperatures is in contrast to the $Hg_{0.79}Cd_{0.21}Te$ data (Fig. 11).

C. Discussion of magnetotransport results

We begin the discussion by noting that for $0.4 \lesssim T \lesssim 77$ K all samples show metallic behavior at $B=0$. This is expected since the donor density is from 10 to 100 times greater than the (zero-field) critical density for the transition given by $n_c^{1/3}a^* \simeq 0.25$. The Bohr radius a^* is ~ 1800 Å (~ 600 Å) for $Hg_{0.8}Cd_{0.2}Te$ (InSb), resulting in $n_c \sim 3\times10^{12}$ cm^{-3} ($\sim 7\times10^{13}$ cm^{-3}). Therefore, for the samples we studied, the magnetic-field-induced M-I transition occurs in the strong-field limit

$$\gamma = \frac{\hbar\omega_c}{2R^*} = (a^*/l)^2 \gg 1 , \tag{2}$$

where $\omega_c = eB/m^*$ is the cyclotron frequency, R^* is the effective donor Rydberg constant, and $l=(\hbar/eB)^{1/2}$ is the magnetic length. Note that $\gamma \sim B$ as indicated on the right-hand side of Fig. 6 for $Hg_{0.8}Cd_{0.2}Te$ and InSb. In the strong-field limit, the characteristic size of the electron wave function (for an isolated hydrogenic donor) in the direction parallel to the field is $a_{\parallel}^* = a^*/\ln\gamma$ and that perpendicular to the field is $a_{\perp}^* = 2l$.[2,41] Thus the volume of the electron wave function is $a_{\parallel}^*(a_{\perp}^*)^2 = [4(a^*)^3]/(\gamma \ln\gamma)$ and decreases as B is raised. Once the overlap between the wave functions of electrons is sufficiently reduced, a M-I transition is expected to occur according to the condition

$$n(a_{\perp}^*)^2(a_{\parallel}) = \delta^3 , \tag{3}$$

where δ is a constant. In Eq. (3) experimental values for the constant δ for many systems of doped semiconductors over a large range of carrier concentrations are found to be in fair agreement with the theoretical estimate $\delta \simeq 0.3$.[41,42]

In order to test the validity of Eq. (3) for the samples we studied, we first determine the fields $B_{M\text{-}I}$ from the onset of the sharp rise in ρ_{xy} data at low temperatures (Figs. 1–3). In Figs. 13 and 14 we show our measured ρ_{xx} and ρ_{xy} for $Hg_{1-x}Cd_xTe$ and InSb samples at temperatures down to 80 mK.[20] Following Refs. 17 and 19 it is possible to extrapolate the apparent onsets of the sharp rise in ρ_{xy} at low temperatures to the $T\rightarrow 0$ limit to extract $B_{M\text{-}I}$. In Ref. 17 it was observed that ρ_{xy} for $Hg_{1-x}Cd_xTe$ exhibited an approximately linear dependence on B for $B > B_{M\text{-}I}$. A temperature-dependent critical field was then defined as the intercept of the linear ex-

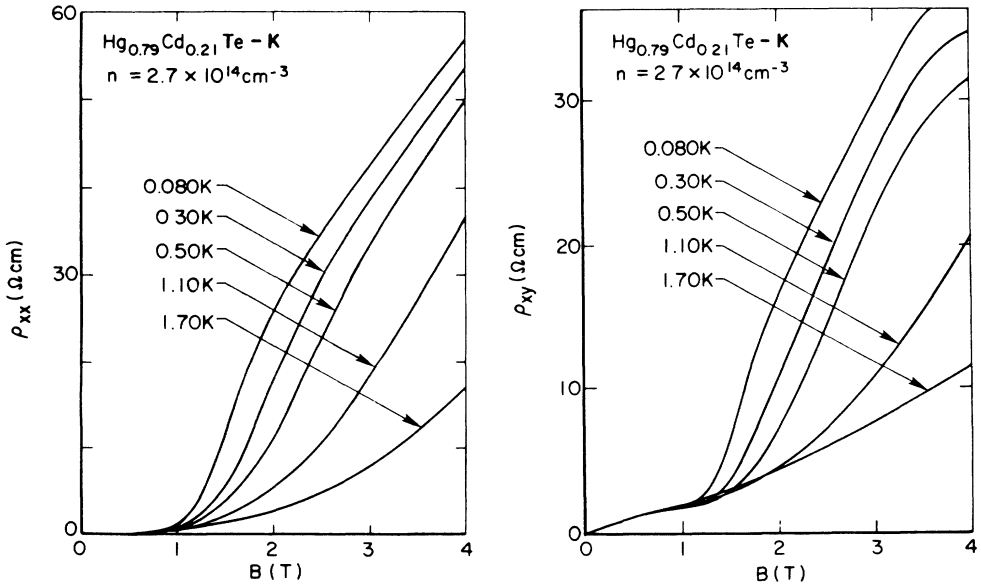

FIG. 13. ρ_{xx} and ρ_{xy} vs magnetic field shown for a $Hg_{0.79}Cd_{0.21}Te$ sample at low temperatures down to 80 mK.

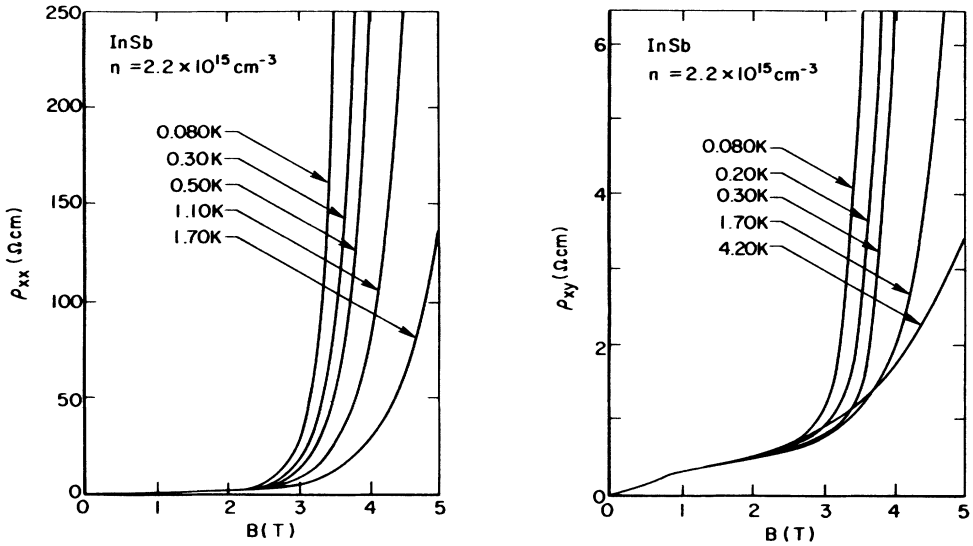

FIG. 14. ρ_{xx} and ρ_{xy} vs B shown for an InSb sample at low temperatures down to 80 mK.

trapolation of ρ_{xy} versus B with the **B** axis.[17] In Ref. 19 it was suggested that a more suitable definition for an apparent characteristic field, associated with the M-I transition at a given T, may be the intercept of the linear extrapolations of ρ_{xy} below and above the abrupt rise in ρ_{xy}. The fields $B_{M\text{-}I}$ in Table I and Fig. 6 were determined by extrapolating these temperature-dependent characteristic fields to the $T\rightarrow 0$ limit. We note that although such an empirical procedure may be useful for determination of $B_{M\text{-}I}$, one should be cautious about the validity of the linear dependence of ρ_{xy} on B, and also of a "critical" field that depends on temperature.[43] We discuss below an alternative determination of $B_{M\text{-}I}$.

We note here that both ρ_{zz} and ρ_{xx} also exhibit a sharp rise at $B_{M\text{-}I}$ (Figs. 1–3, 13, and 14), although their temperature dependence starts at magnetic fields below $B_{M\text{-}I}$ (see below). Similar behavior was observed for InSb (Ref. 44) and GaAs,[29,45] and was interpreted in terms of effects due to electron-electron correlation and disorder. It is expected from the theory of disordered metals in weak magnetic fields[46] that the temperature dependence of the longitudinal conductivity σ_{zz} $(=\rho_{zz}^{-1})$ in the vicinity of the M-I transition is given by

$$\sigma_{zz}(T)=\sigma_0+AT^{1/2}+CT\ , \tag{4}$$

where σ_0, A, and C are constants. In Eq. (4) the $AT^{1/2}$ term is due to Coulomb interaction and the CT term is due to weak localization effects.[46] For magnetic fields greater than $B_{M\text{-}I}$, $\sigma_0=0$. Although the validity of Eq. (4) in the presence of a strong magnetic field is not theoretically confirmed, such an expression has been used to interpret the experimental data.[29,44,45]

In Fig. 15 we show σ_{zz} for a $Hg_{1-x}Cd_xTe$ and an InSb sample as a function of $T^{1/2}$. These data are qualitatively similar to the data of Ref. 44 on InSb, and can be fitted to Eq. (4) fairly well. In fact, the M-I transition field $B_{M\text{-}I}$ can be determined from Fig. 15 as the field above which σ_0, used to fit Eq. (4) to the data, vanishes. We found $B_{M\text{-}I}\simeq 1.1$ T for the $Hg_{0.79}Cd_{0.21}Te$ sample and $B_{M\text{-}I}\simeq 3.2$ T for the InSb sample of Fig. 15, in good agreement with $B_{M\text{-}I}$ determined from the Hall data (Table I). We estimate the accuracy of the fields $B_{M\text{-}I}$ in Table I and Fig. 6 to be $\pm 10\%$. The solid curves in Fig. 6 represent the critical field versus density calculated using Eq. (3). The constant δ was chosen to be 0.31 (0.34) for $Hg_{0.8}Cd_{0.2}Te$ (InSb). These values are in fair agreement with the theoretical estimate ($\delta\simeq 0.3$) and previous experimental results.[47]

We now focus on the anomalous "Hall dip" below $B_{M\text{-}I}$, and interpret it in terms of a model based on a tight-binding approach to the donor band in the vicinity of the M-I transition.[22] The model assumes that a semiconductor crystal contains an infinite metallic donor cluster as well as shallow donors which do not have close neighbors thus supporting effectively localized electronic states. The average carrier concentration in the infinite cluster is greater than the crystal-average electron concentration.

In the tight-binding picture the amplitude of the electron wave-function peaks on the donor sites and the metallic electrical conduction via the impurity band (in the limit $T\rightarrow 0$) involves tunneling (not hopping) from an occupied to a neighboring unoccupied donor. Still on the metallic side, but not far from the transition, the crystal contains an infinite metallic donor cluster[48] as well as regions which do not participate in the electrical transport, i.e., are insulating. For example, a donor which does not have any other donor closer than some distance b supports an effectively localized electronic state[49] for b large enough that the overlap integral of this state with the metallic states is exponentially small. Tunneling through the regions of the crystal containing such a donor is not feasible since it involves large distances.

For randomly placed donors the probability density for

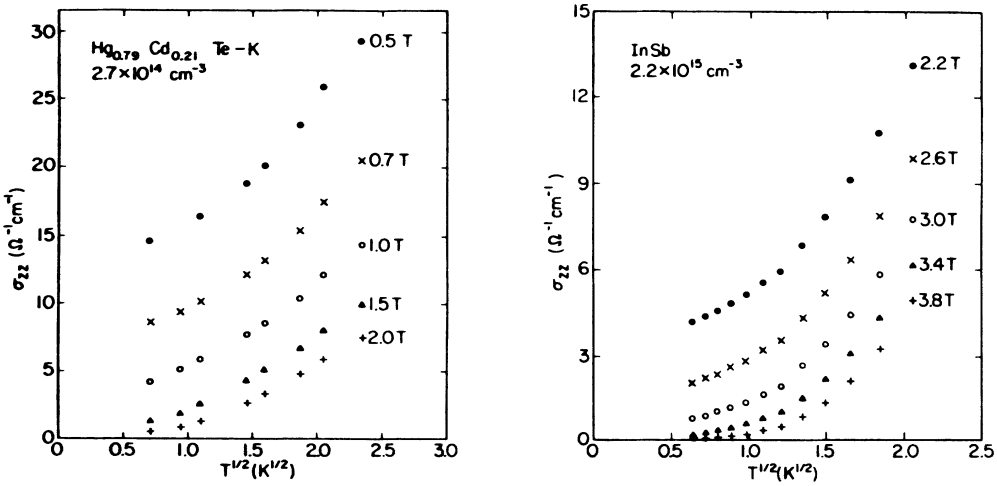

FIG. 15. Plots of the longitudinal conductivity σ_{zz} vs $T^{1/2}$ shown for $Hg_{0.79}Cd_{0.21}Te$ and InSb. The metal-insulator transition field $B_{M\text{-}I}$ can be determined as the field above which σ_0 used to fit Eq. (4) to this data vanishes. $B_{M\text{-}I} \simeq 1.1$ T ($\simeq 3.2$ T) was determined for the $Hg_{0.79}Cd_{0.21}Te$ (InSb) samples, respectively.

a donor to have the nearest neighbor at distance r is given by the Poisson formula

$$P(r)=r^2/(3r_D^3)\exp[-(r/r_D)^3] ,$$

where $r_D^3=3/(4\pi N_D)$ and N_D is the donor concentration. Therefore, the concentration of the donors which have no other donor closer than b is

$$\Delta n(b)=n\int_b^\infty P(r)dr = n\exp[-(b/r_D)^3] . \quad (5)$$

If we assume that each such isolated occupied donor excludes a volume of $4\pi r^3/3$ from the infinite metallic cluster, the fraction of the volume of the crystal excluded from electrical conduction is

$$\varepsilon(b)=n\int_b^\infty (4\pi r^3/3)P(r)dr$$

$$=[(4\pi b^3)/(3r_D^3)+1]\exp[-(b/r_D)^3] . \quad (6)$$

The conduction takes place in the infinite metallic cluster of the average donor concentration

$$n_{\text{eff}}(b)=\frac{n-\Delta n(b)}{1-\varepsilon(b)} . \quad (7)$$

Since every isolated donor takes up one electron from the metallic cluster and excludes a volume greater than the average volume per electron, n_{eff} is greater than n. It is known that the Hall coefficient of a macroscopically inhomogeneous material treated within the effective-medium theory $R_H=h/n_{\text{eff}}e$, where h is a geometrical factor.[50,51] However, it can be argued that in the case of *microscopic* inhomogeneities, when the electron-scattering length is on the order of, or even greater than, the size of typical inhomogeneity, $h \simeq 1$.[52]

We now apply these results to the narrow-band-gap semiconductors in a magnetic field. We use the expressions for the characteristic size of the electron wave function in the strong-field limit, i.e., $a_\parallel^*=a^*/\ln\gamma$ and $a_\perp^*=2l$. Thus $a_\parallel^*(a_\perp^*)^2=[4(a^*)^3]/(\gamma\ln\gamma)$ and decreases as B is raised. Expressing b in Eqs. (5)–(7) in units of $a_\parallel^*(a_\perp^*)^2$, that is $b^3=Ma_\parallel^*(a_\perp^*)^2$, in the strong-field limit ($\gamma \gg 1$), and using $h=1$, we obtain

$$R_H(B)=\frac{1}{en_{\text{eff}}(B)}=\frac{1-\varepsilon(B)}{e[n-\Delta n(B)]} . \quad (8)$$

M is a dimensionless parameter; within our model if a donor does not have a neighbor in the volume $[4\pi Ma_\parallel^*(a_\perp^*)^2]/3$, it does not participate in electrical conduction at $T\to 0$.

In Fig. 16 we show the Hall coefficient R_H [normalized to R_H $(B\to 0)$] for a $Hg_{0.8}Cd_{0.2}Te$ sample (P in Table I) at the lowest experimental temperature. Figure 16 also shows a fit based on Eq. (8) with M used as a fitting parameter. The theoretical curve shown has $M=12$; this means that the microscopic M-I transition criterion (on the scale of a few donors) is $na_\parallel^*(a_\perp^*)^2 \simeq 3/(4\pi M) = (0.27)^3$, in contrast to the macroscopic (on the scale of the whole crystal) Mott criterion $na_\parallel^*(a_\perp^*)^2 \simeq (0.31)^3$ (see Fig. 6). This difference of the microscopic and the macroscopic Mott criteria is consistent with the picture of the macroscopic M-I transition in crystalline semiconductors being a percolation threshold of formation of the infinite metallic donor cluster. It is clear that our model applies only to the metallic side and not to the insulating side of the M-I transition (i.e., it does not apply to the range $B \geq B_{M\text{-}I}$).

Figure 17 shows the normalized $R_H(B)$ data for several other $Hg_{1-x}Cd_xTe$ and the InSb samples. The horizontal axis is $(\gamma\ln\gamma)/[n(a^*)^3]$ in order to scale the data for different samples in accordance with Eq. (8) in the region of strong fields. The scatter of the experimental curves is on the order of the accuracy with which the samples' parameters (n, m^*, κ) are known. The common fit of Eq. (8) is the same as in Fig. 16 ($M=12$). We note here that for the InSb samples $B_{M\text{-}I}$ corresponds to $\gamma \lesssim 30$; therefore, the high-field limit is not fully applicable. This may be the cause of the worse scaling of InSb data in Fig. 17.[53]

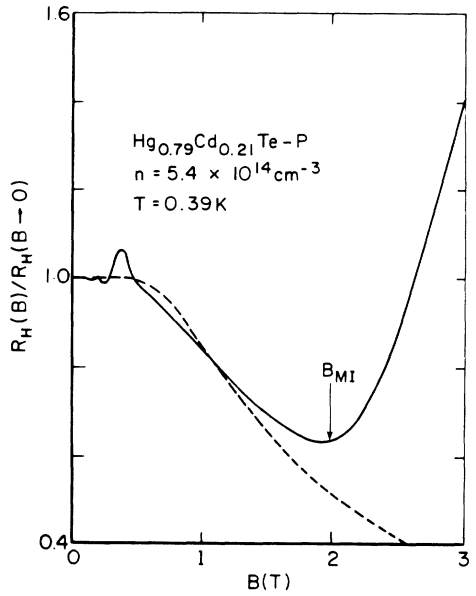

FIG. 16. Normalized Hall coefficient of a $Hg_{0.79}Cd_{0.21}Te$ sample (P) as a function of the magnetic field. The "Hall-dip" region extends from the last magnetoquantum oscillation to $B_{M\text{-}I} \simeq 2.0$ T ($\gamma = 100$). The dashed line gives a fit based on Eq. (8) (see text). The fit does not apply for $B \gtrsim B_{M\text{-}I}$.

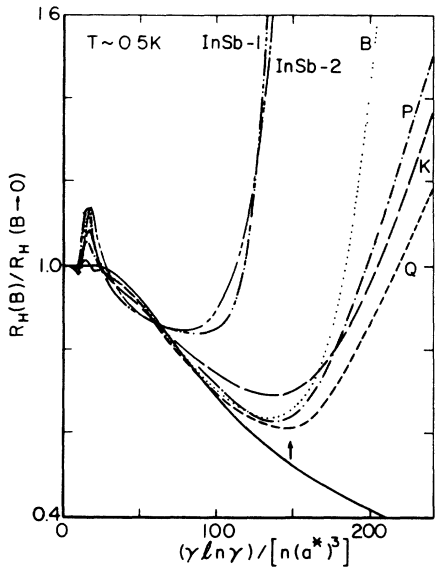

FIG. 17. The normalized Hall coefficients of several $Hg_{0.79}Cd_{0.21}Te$ and InSb samples vs $(\gamma \ln\gamma)/[n(a^*)^3]$. The densities of the samples are given in Table I. The fit of Eq. (8) is with the same parameter $M = 12$ as in Fig. 16. The arrow indicates the M-I transition according to the condition $na_{\|}^*(a_{\perp}^*)^2 = (0.31)^3$.

The reasonable scaling of the Hall data for the $Hg_{1-x}Cd_xTe$ samples with n spanning an order of magnitude is in itself evidence for the impurity-band nature of the conduction near the M-I transition (the scaling involves the shallow-donor effective Bohr radius). Our model does not take into account several factors that may play an important role in the electrical transport near the M-I transition. We neglected the influence of compensation (except as mentioned in Ref. 28), the effects of finite temperatures, and the electron-electron interaction.[54] The calculation does not take into account the presence of isolated donor doublets and more complex clusters. Also, we spherically averaged the donor distribution although the magnetic field reduces the symmetry to only cylindrical. The geometrical factor h most likely deviates noticeably from the value of 1 we used (especially close to the M-I transition), thus increasing $R_H(B)$ and producing the rounding at fields close to $B_{M\text{-}I}$ as is evident in experimental curves.[55]

We believe that our model explains the presence, the direction and the magnitude of the "Hall dip." A more accurate and involved calculation would produce qualitatively similar results, probably leading to an increased value of M since it would take into account more complex isolated donor clusters. We consider the general agreement of Eq. (8), derived within a very simple model, and the experiment as encouraging and strong evidence for the appropriateness of the tight-binding approach to the impurity-band problem in crystalline semiconductors.

D. Is there evidence for Wigner crystallization of electrons in $Hg_{1-x}Cd_xTe$?

Certain anomalous features in the magnetotransport data of $Hg_{1-x}Cd_xTe$ have been interpreted in the past as evidence for Wigner crystallization of electrons in this material. We review some of these features here and compare them with our data.

(1) In Refs. 8 and 14–16 it was reported that the Hall coefficient R_H does not rise appreciably at magnetic fields above $B_{M\text{-}I}$. A temperature-dependent ρ_{zz}, however, was observed and was interpreted as evidence for an activated mobility. It was concluded that the system could be described as a highly correlated electron liquid and/or a Wigner crystal. Our data (Figs. 2, 3, 7, 13, and 18) indicate that, at low temperatures, ρ_{xy} sharply rises at magnetic fields above $B_{M\text{-}I}$. This behavior is similar to what is observed in InSb (see, e.g., Fig. 1), and is consistent with the magnetic-field-induced freeze-out effect. It was recently argued that an improper sample geometry (small length-to-width ratio L/W) is responsible for our observation.[56] Considering the geometry of our samples (see Sec. III A), and also the fact that a temperature dependent R_H was indeed observed by other groups[17] we believe that our measurements do give the Hall resistivity correctly.[57]

(2) We mentioned earlier that in view of the similarity of the electronic structure of $Hg_{1-x}Cd_xTe$ to that of InSb, the similarity between the transport data as well as the magnetooptical properties of these semiconductors is expected. It has been argued, however, that unlike the case of InSb, the conduction-band electrons in bulk n-type $Hg_{1-x}Cd_xTe$ are derived from Te vacancies and that this difference is responsible for the absence of magnetic freeze-out in $Hg_{1-x}Cd_xTe$.[8,14–16,40] Dornhaus *et al.*[40] claimed to have observed a donor state above the bottom of the conduction band which they *assumed* to be created by Te vacancies. The evidence for this resonant level was reported to be an anomalous peak in the magne-

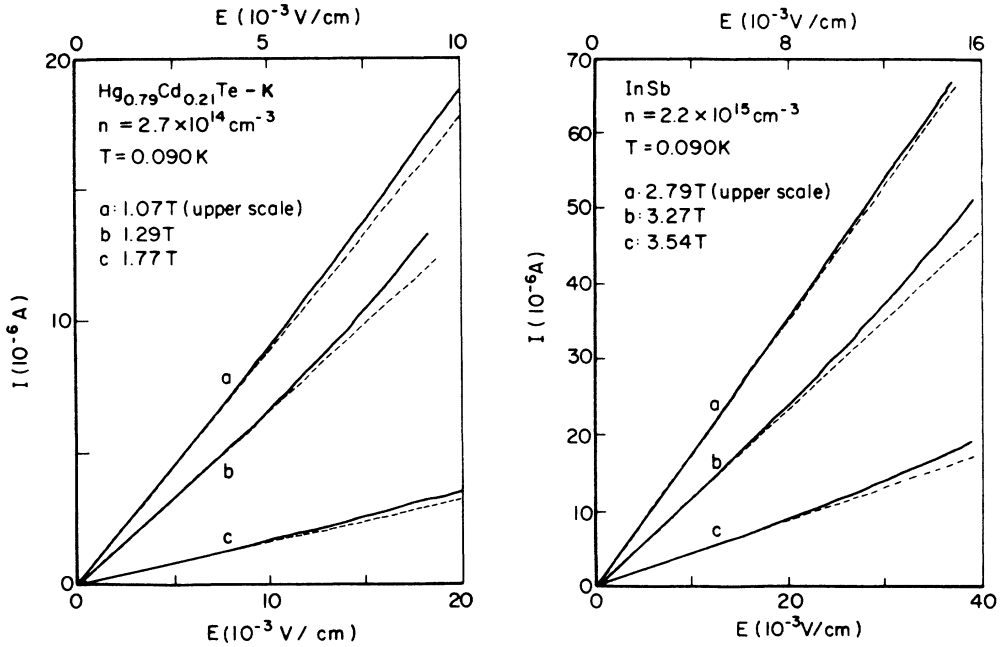

FIG. 18. The current vs electric field (I-E) characteristics, measured for the transverse resistivity, shown by solid curves for $Hg_{0.79}Cd_{0.21}Te$ (InSb) for three magnetic fields near the metal-insulator transition field $B_{M\text{-}I} \simeq 1.1$ T (3.2 T). The bath temperature was held constant at 0.090 K. For each sample, the scale for curves a is indicated on top of the figure while b and c have the bottom scale. The dashed curves are expansions (by a factor of 3) of the low-electric-field portions of the solid curves.

totransport data which shifted to lower magnetic fields as a function of increasing carrier density.[40] We note in Figs. 4–6 that no such anomalous feature was observed in any of our samples. In addition, even if such a resonant state exists and a level crossing occurs, the electrons would occupy the "Te-vacancy" states and a total free-carrier freeze-out follows (contradictory to the reported Hall data of Refs. 8 and 14–16). Moreover, vacancy-derived free carriers would be no more susceptible to Wigner crystallization than those derived from substitutional donors. Any point-defect source of free electrons must leave behind fixed positive charge and, therefore, supports shallow levels.

(3) Weak dependencies of the resistivities in $Hg_{1-x}Cd_xTe$ on the magnetic field at high fields and low temperatures was reported several years ago as evidence for Wigner crystallization of electrons.[8,14] More recently, Rosenbaum *et al.* interpreted the nonactivated behavior of ρ_{xy} above $B_{M\text{-}I}$, and the apparent linear dependence of $B_{M\text{-}I}$ on temperature as evidence for the melting transition of a Wigner crystal.[17] As noted earlier, such anomalous data should be interpreted with extreme care in view of the conducting surface layer in $Hg_{1-x}Cd_xTe$.[58] Moreover, neither a weak magnetoresistance nor a nonactivated ρ_{xy} can by themselves be regarded as evidence in favor of a Wigner crystal.

(4) Recently, non-Ohmic behavior in a $Hg_{0.76}Cd_{0.24}Te$ sample at high magnetic fields above $B_{M\text{-}I}$ was reported by Field *et al.*[17] They observed nonlinearity in ρ_{zz} starting at very low electric fields of the order of 0.5 mV cm^{-1} which they interpreted as evidence for the depinning of a Wigner crystal. In our measurements of the transverse resistivity ρ_{xx}, we observed a non-Ohmic behavior in both $Hg_{1-x}Cd_xTe$ and InSb starting at electric fields an order of magnitude higher than 0.5 mV cm^{-1}. Field *et al.* also reported another nonlinearity at higher electric fields (comparable to those reported here) and attributed it to sample heating.[17] Considering the small activation energies involved for barely insulating samples, thermally assisted impact ionization and other hot electron effects cannot be ruled out and may account for the observed non-Ohmic behavior.[59]

(5) Finally, Stadler *et al.* recently reported measurements of the energy relaxation time τ_ε for hot electrons in n-type $Hg_{0.8}Cd_{0.2}Te$ in quantizing magnetic fields.[16] Using a simplified energy-balance equation, they deduced the heat capacity C_v of the hot-electron system from the dependence of τ_ε on the electron "effective temperature" T_e. They interpreted a broad and shallow peak in C_v at $T_e \sim 2$ K and the falloff of C_v below this temperature as evidence that the system goes through a magnetic-field-induced liquidlike phase and into a Wigner crystal at low temperatures. We have pointed out[60] that the data presented in Ref. 16 do not provide evidence for Wigner crystallization of electrons in this material. Rather, the data indicate that there is a decrease of τ_ε and C_v, as calculated in Ref. 16, with decreasing T_e as T_e approaches the lattice temperature T_L ($T_L = 1.5$ K in Ref. 16). Similar measurements of τ_ε versus T_e on insulating InSb made at zero magnetic field and at different T_L show essentially the same behavior.[61–63] Therefore, in Ref. 16 the primary significance of the temperature range 1.5–1.9 K where C_v rapidly decreases, we believe, is that it lies just above the experimental T_L. The falloff of C_v in this

range, therefore, does not provide evidence for the formation and/or melting of a Wigner crystal. Also, Aronzon, Kopylov, and Meilikhov[64] very recently studied the electronic specific heat near the *M-I* transition in *n*-type $Hg_{0.8}Cd_{0.2}Te$ using a method similar to that of Ref. 16. They did not, however, find any singularity in the specific heat at the *M-I* transition field and associated the transition with Anderson localization in potential fluctuations.[64]

E. Summary and conclusions

The low-temperature magnetotransport data presented in this section establish the basic similarity between the magnetic-field-induced *M-I* transitions in InSb and $Hg_{1-x}Cd_xTe$. We find this identity intuitively appealing, considering the fact that the electronic structures of these narrow-band-gap semiconductors are very similar. The agreement of the transport data with the proposed model provides evidence that the magnetic-field-induced *M-I* transition in $Hg_{1-x}Cd_xTe$ and InSb occurs in the impurity band and is not a manifestation of Wigner crystallization of electrons.

IV. IMPURITY CYCLOTRON RESONANCE IN $Hg_{1-x}Cd_xTe$

Impurity cyclotron resonance (ICR) is an optically induced transition of a donor-bound electron from the ground state, related to the lowest ($N=0$, spin-up) Landau-level states, to an excited bound state, related to the $N=1$, spin-up Landau level. The energy separation of the donor-bound states is slightly greater than that of the Landau levels and, therefore, ICR is shifted from the free-carrier resonance. The first observation of impurity cyclotron resonance was reported for InSb in 1957,[65] and this phenomenon has been studied extensively since then.[4-6]

Here we report on the observation of ICR in $Hg_{1-x}Cd_xTe$—the first conclusive evidence, to our knowledge, that at low enough temperatures and sufficiently high magnetic fields the conduction-band electrons are bound on donors.[21] The energy splitting between the ICR and the conduction-band cyclotron resonance (CCR) is consistent with calculations performed within the hydrogenic donor model[66,67] and can be used to determine the binding energy of the electrons. The saturation of the ICR absorption with the incident radiation intensity, previously studied in InSb,[5,6] was used here to measure the lifetime of the electrons accumulating in the lowest Landau level; we found $T_1 \sim 10^{-6}$ s—nearly 2 orders of magnitude longer than in InSb.

Samples (*H* and *Y* in Table I) were cut from 15-mm diam wafers, thinned, polished, and briefly etched in a 3% bromine-methanol solution minutes before mounting in the cryostat.[68] Final thicknesses were $d=305$, 290, and 260 μm for samples *Ha*, *Hb*, and *Y*, respectively. Measurements were made in Faraday configuration using far-infrared (fir) radiation from an optically pumped cw laser. The radiation was circularly polarized using a fir linear polarizer and a crystal quartz $\lambda/4$ plate, and was detected by a Ge:Ga composite bolometer. The samples were mounted on a wedged germanium substrate and were immersed in pumped liquid ^{4}He to achieve temperatures below 4 K. A fir absorber with a small, 3-mm-diam hole was placed immediately in front of the samples to ensure the uniformity of the incident radiation.

Typical magnetotransmission spectra are shown in Fig. 19. The ICR absorption decreases and the CCR absorption increases as the temperature [Fig. 19(a)] or the radia-

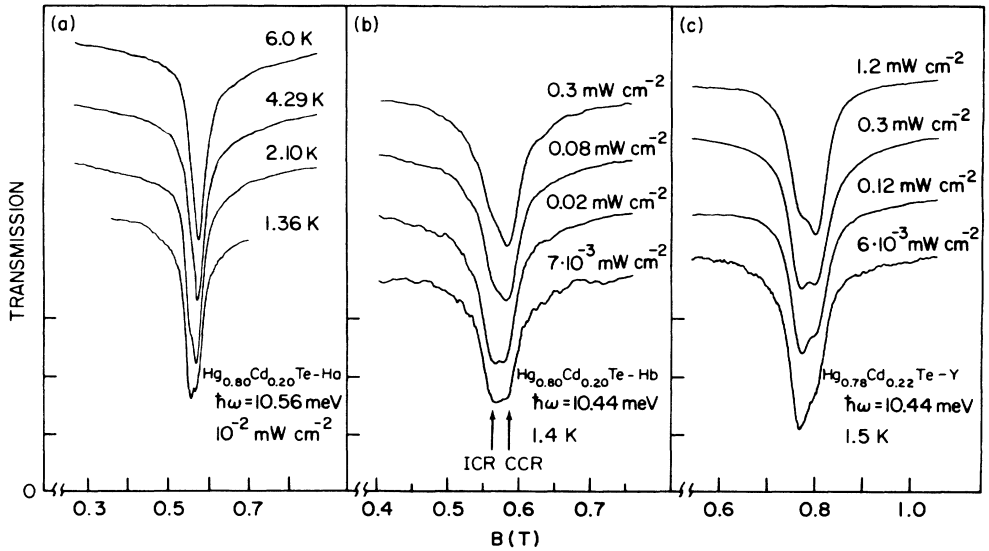

FIG. 19. Magnetotransmission spectra of *n*-type $Hg_{1-x}Cd_xTe$ samples at different temperatures and fir radiation intensities. The arrows show the absorption-peak assignment. Zero transmission levels, corrected to 100% cyclotron-resonance-active circular polarization, are shown by horizontal tick marks on the left-hand axis for each respective trace.

tion intensity [Figs. 19(b) and 19(c)] is raised. There is no ICR absorption in the cyclotron-resonance-inactive circular polarization within the experimental uncertainty of $\sim 2\%$, in agreement with the theoretical prediction[66] that the selection rules for the two processes are the same.

From the transmission data we calculated αd, where $\alpha(B)$ is the absorption coefficient and d is the sample thickness. We neglected multiple reflections because of the substrate. At high temperatures (~ 10 K) where only CCR is present, the data can be fitted reasonably well with a Lorentzian absorption line, which indicates high compositional uniformity of the samples. The linewidth is consistent with the 77-K Hall mobility. From the low-temperature experimental absorption we substract a Lorentzian line with the resonance field, $B_{\rm CCR}$, and the half-width, Γ, from the high-temperature fit and use the peak CCR absorption, α_C, as a fitting parameter to get a smooth, approximately Lorentzian ICR absorption (cf. Fig. 20).[69] We estimate the resulting uncertainty in the resonance field splitting, $B_{\rm CCR}-B_{\rm ICR}$, as 2.5 mT for $x=0.224$ and 1.5 mT for $x=0.204$. The peak absorption $\alpha_I d$ is accurate to within 5–10 %.

The resonance fields, $B_{\rm CCR}$ and $B_{\rm ICR}$, are plotted versus photon energy, $\hbar\omega$, in Fig. 21(a); the lines show a nonparabolic, Bowers-Yafet model[70] calculation with the band-bottom effective mass, $m^*(B=0)$, used as a fitting parameter. The energy splitting between the ICR and CCR,[71] $\Delta \equiv (E_{110}-E_{000})-(E_{1^+}-E_{0^+})$, was calculated from

$$\Delta(B) \simeq [d(E_{1^+}-E_{0^+})/dB]_{B=B_{\rm CCR}}(B_{\rm CCR}-B_{\rm ICR}) ,$$

and is shown in Fig. 21(b). The lines in Fig. 21(b) give results of Larsen's nonparabolic model calculation,[67] adapted for our samples by using m^* given in Fig. 21(a) and the static dielectric constant $\kappa=17$. In the experimental range of magnetic fields, the data are in qualitative agreement with the theory[67] developed for an isolated donor. The quantitative discrepancy ($\sim 20\%$) is similar to that observed in InSb samples.[4,72]

Figure 22 gives the dependence of the peak ICR absorption, $\alpha_I d$, on the fir radiation intensity I. A three-level model[5] predicts

$$\frac{\alpha_I(I)}{\alpha_I(0)} = \left[1+\frac{\alpha_I(0)I}{\hbar\omega n}T_1\right]^{-1} , \tag{9}$$

where T_1 is related to the electronic lifetime of the 0^+ Landau level. In this model the electrons are excited by the fir radiation from (000) state to (110) state from which they relax to the 0^+ level and directly to the ground state (000) with time constants τ_{32} and τ_{31}, respectively. Denoting the lifetime of the 0^+ Landau level by τ_{21} and making the same assumptions as Ref. 6 ($\tau_{32} \ll \tau_{31}$, $\tau_{32} \ll \tau_{21}$) at low enough temperatures, $T_1 \simeq \tau_{21}$.

The reported lifetimes[5,6] for InSb fit the empirical relation $T_1 \simeq 2.5\times 10^{-9}\gamma$ s, where $\gamma \equiv (a^*/l)^2$ and the magnetic length $l=(\hbar/eB)^{1/2}$. For samples Y and Hb we ob-

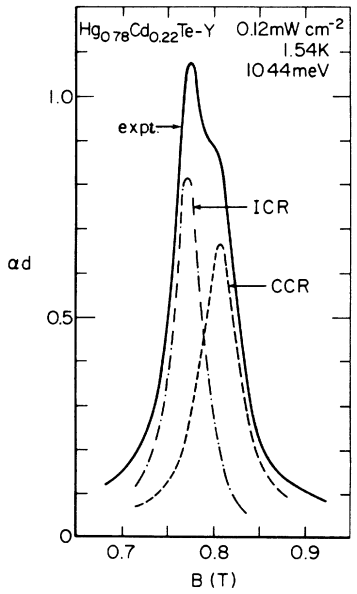

FIG. 20. Example of fir absorption analysis (described in the text). About 10 magnetotransmission spectra at different intensities were used at every photon energy to obtain a pair of data points in Fig. 21 and the experimental uncertainties given in the text.

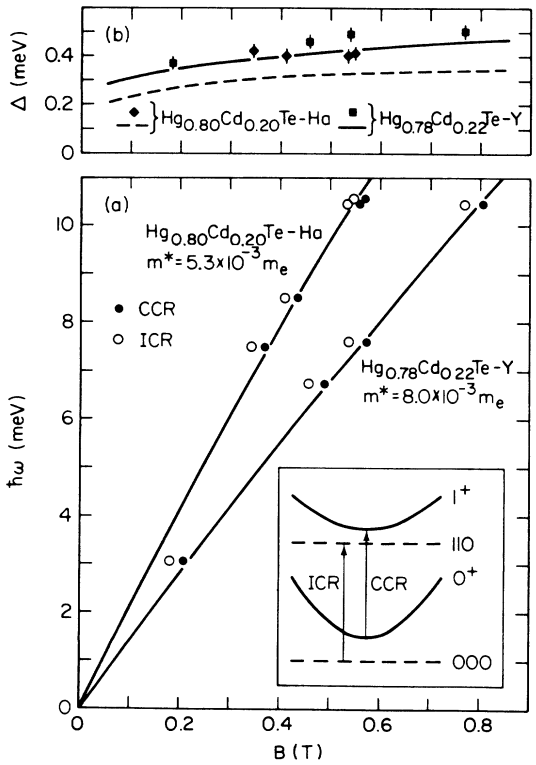

FIG. 21. (a) Resonance magnetic fields at several fir photon energies $\hbar\omega$. The lines give nonparabolic fits for $0^+ \rightarrow 1^+$ transition, with m^* used as fitting parameter. The inset shows the relevant energy-level scheme. (b) The energy splitting $\Delta=\hbar\omega_{\rm ICR}-\hbar\omega_{\rm CCR}$ vs magnetic field. The lines show scaled theoretical prediction of Ref. 67. Effective Rydbergs for samples Ha and Y are, respectively, 0.25 and 0.38 meV.

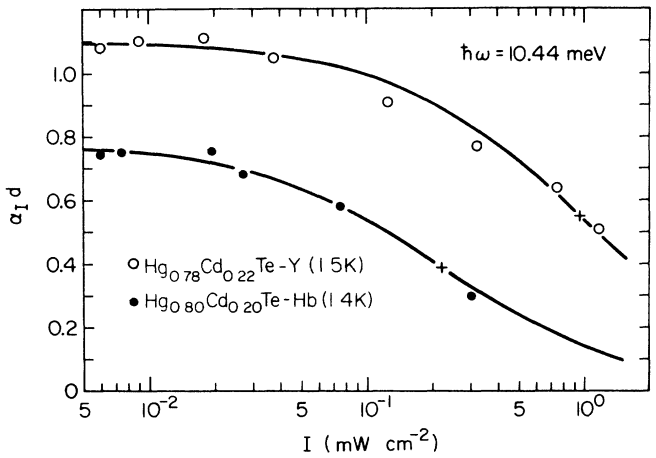

FIG. 22. Measured peak ICR absorption of the samples as a function of fir radiation intensity. The curves are fits of Eq. (9) with the sample parameters given in Table I and in the text. Pluses denote intensities $I_{1/2}$ such that $2\alpha_I(I_{1/2})=\alpha_I(0)$. The fits give times $T_1=3.4\times10^{-6}$ and 1.6×10^{-6} s for samples *Hb* and *Y*, respectively.

tained $T_1\simeq1.0\times10^{-7}\gamma$ s and $1.4\times10^{-7}\gamma$ s, respectively. These are substantially longer lifetimes than for InSb. We believe that the relative uncertainty in values of I is $\sim10\%$; however, the absolute calibration of fir intensity is accurate only to within a factor of 2. A more extensive study in this alloy semiconductor can determine the band-gap and/or effective-mass dependence of the inelastic lifetime of the lowest Landau level and the chemical shifts[72] in the donor binding energies.

Several factors combine to make the experimental observation of ICR and data analysis more difficult for $Hg_{0.8}Cd_{0.2}Te$ than for InSb. Lower electron effective mass and low $\hbar\omega_{LO}=17$ meV limit the measurements to lower magnetic fields, which, in turn, combined with smaller effective Rydberg, leads to smaller relative splitting between ICR and CCR and requires lower experimental temperatures and impurity concentrations. The alloy potential fluctuations may broaden both ICR and CCR. In addition, the surface of $Hg_{1-x}Cd_xTe$ attracts electrons from the bulk. We have performed a study of this phenomenon using CR absorption to determine the fraction of the electrons left in the bulk. It has been found that with our sample-preparation procedure the bulk electron per square concentration decreased linearly with the sample's thickness as $N=nd-N_s$, where $N_s\simeq6\times10^{11}$ cm^{-2} was concluded to be the surface electron density. Since the width of CCR did not change appreciably as a sample was thinned, down to $N\simeq3\times10^{10}$ cm^{-2}, we also concluded that the bulk concentration, n, does not change, but rather that the surface electrons leave behind depletion layers, at each side of the sample.

We note here that the cyclotron resonance of an accumulation layer would be shifted to higher fields due to nonparabolicity and, more important, would be much broader than the bulk CCR due to the high scattering rate of the surface electrons. We do observe a weak and broad background absorption in the magnetotransmission data which can be due to the surface-bound electrons.

Shorting of the bulk by the surface conduction prevented us from obtaining useful transport data in these low-n samples. However, by extrapolation from the data on higher-n samples, we can estimate that the magnetic-field-induced metal-insulator transition field, $B_{M\text{-}I}$, for sample *Y* is approximately 0.35 T. The fir data at $\hbar\omega=2.99$ meV show the ICR absorption present at a lower field (cf. Fig. 23) with the integrated absorption strength equal to that at higher fields, within the experimental uncertainty. This experimental observation does not fit into any of the *M-I* transition pictures mentioned in the Introduction and suggests that even on the metallic side of the *M-I* transition the delocalized electrons are in donor band states which are distinct from the conduction-band states.

V. SUMMARY AND CONCLUSION

We believe that the selection rules, the magnitude of the splitting, and its magnetic field dependence together with the absorption saturation effect allow us to identify the low-field peak in the magnetotransmission spectra of $Hg_{1-x}Cd_xTe$ as the (000)→(110) ICR transition, which is direct and conclusive evidence for hydrogenic donors in this material. This has been further confirmed by recent Voigt-geometry measurements of the (000)→(0$\bar{1}$1) transitions in $Hg_{1-x}Cd_xTe$.[24,73] This observation allows us to conclude that the Wigner condensation of the conduction-band electrons does not occur in $Hg_{1-x}Cd_xTe$. The observed similarity of the magnetotransport data for $Hg_{1-x}Cd_xTe$ and InSb in the vicinity of the magnetic-field-induced *M-I* transition further confirms this conclusion. Both the observation of ICR at magnetic fields below the *M-I* transition, and the agreement of the transport data with the proposed model, suggest that the magnetic-field-induced *M-I* transition in these narrow-band-gap semiconductors takes place in the donor impurity band.

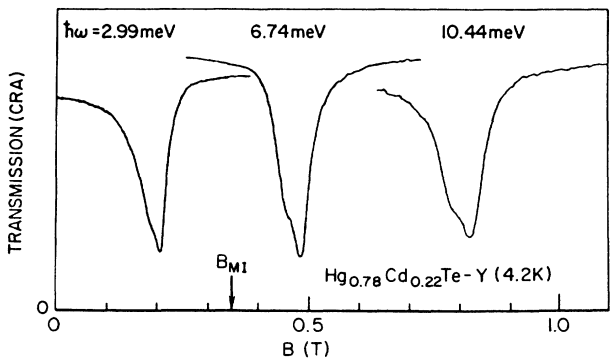

FIG. 23. Magnetotransmission spectra of a $Hg_{0.78}Cd_{0.22}Te$ sample (*Y*) at different fir wavelengths [cyclotron-resonance-active (CRA) circular polarization] showing the presence of ICR at magnetic fields below $B_{M\text{-}I}$.

ACKNOWLEDGMENTS

Part of this work was performed at the Francis Bitter National Magnet Laboratory, which is supported at MIT by the National Science Foundation. We thank D. A. Nelson for the $Hg_{1-x}Cd_xTe$ samples, and B. Brandt, J. S. Brooks, N. A. Fortune, L. Rubin, and P. M. Tedrow for technical assistance. We acknowledge support through National Science Foundation (NSF) Grants No. ECS-85-53110 and No. DMR-87-05002 for one of us (M.S.) and NSF Grant No. DMR-87-04670 and U.S. Office of Naval Research (ONR) Grant No. N00014-86-K-0273) for another (H.D.D.).

[1]See, e.g., A. H. MacDonald and G. Bryant, Phys. Rev. Lett. **58**, 515 (1987), and references therein; B. I. Halperin, Jpn. J. Appl. Phys. **26**, Suppl. 26-3, 1913 (1987).

[2]Y. Yafet, R. W. Keyes, and E. N. Adams, J. Phys. Chem. Solids **1**, 137 (1956); R. W. Keyes and R. J. Sladek, *ibid.* **1**, 143 (1956).

[3]See, e.g., S. Ishida and E. Otsuka, J. Phys. Soc. Jpn. **42**, 542 (1977); **43**, 124 (1977); **46**, 1207 (1979); H. Tokumoto, R. Mansfield, and M. J. Lea, Philos. Mag. B **46**, 93 (1982).

[4]R. Kaplan, Phys. Rev. **181**, 1154 (1969); E. J. Johnson and D. H. Dickey, Phys. Rev. B **1**, 2676 (1970); F. Kuchar, E. Fantner, and G. Bauer, J. Phys. C **10**, 3577 (1977).

[5]T. Murotani and Y. Nisida, J. Phys. Soc. Jpn. **32**, 986 (1972); K. L. I. Kobayashi and E. Otsuka, J. Phys. Chem. Solids **35**, 839 (1974).

[6]E. Gornik, T. Y. Chang, T. J. Bridges, V. T. Nguyen, and J. D. McGee, Phys. Rev. Lett. **40**, 1151 (1978); W. Muller, E. Gornik, T. J. Bridges, and T. Y. Chang, Solid State Electron. **21**, 1455 (1978).

[7]For a review, see C. M. Care and N. H. March, Adv. Phys. **24**, 101 (1975).

[8]G. Nimtz, B. Schlicht, E. Tyssen, R. Dornhaus, and L. D. Haas, Solid State Commun. **32**, 669 (1979).

[9]A. Raymond, J. L. Robert, R. L. Aulombard, C. Bousquet, O. Valassiades, and M. Royer, in *Physics of Narrow Gap Semiconductors,* Vol. 152 of *Lecture Notes in Physics,* edited by E. Gornik *et al.* (Springer-Verlag, Berlin, 1982), p. 387.

[10]G. De Vos and F. Herlach, in *Physics of Narrow Gap Semiconductors,* Ref. 9, p. 377; also in *Application of High Magnetic Fields in Semiconductor Physics,* Vol. 177 of *Lecture Notes in Physics,* edited by G. Landwehr (Springer-Verlag, Berlin, 1983), p. 378; G. De Vos, F. Herlach, and W. W. Myron, J. Phys. C **19**, 2509 (1986); F. Herlach and G. De Vos, J. Phys. C **20**, 5901 (1987).

[11]Yu. G. Arapov, A. B. Davydov, M. L. Zverva, V. I. Stafeev, and L. M. Tsidil'kovskii, Fiz. Tekh. Poluprovodn. **17**, 1392 (1983) [Sov. Phys.—Semicond. **17**, 885 (1983)].

[12]I. M. Tsidil'kovskii, Yu. G. Arapov, A. B. Davydov, and M. L. Zvereva, Pis'ma Zh. Eksp. Teor. Fiz. **44**, 80 (1986) [JETP Lett. **44**, 101 (1986)].

[13]A. B. Aleinikov, P. I. Baranskii, and A. V. Zhidkov, Pis'ma Zh. Eksp. Teor. Fiz. **35**, 464 (1982) [JETP Lett. **35**, 575 (1982)]; Solid State Commun. **48**, 75 (1983).

[14]G. Nimtz and B. Schlicht, in *Festkörperprobleme (Advances in Solid State Physics),* edited by J. Treusch (Vieweg, Braunschweig, 1980), Vol. 20, p. 369; B. Schlicht and G. Nimtz, in *Physics of Narrow Gap Semiconductors,* edited by E. Gornik *et al.* Ref. 9, p. 383; J. Gebhardt, G. Nimtz, B. Schlicht, and J. P. Stadler, Phys. Rev. B. **32**, 5449 (1985).

[15]J. P. Stadler, G. Nimtz, B. Schlicht, and G. Remenyi, Solid State Commun. **52**, 67 (1984).

[16]J. P. Stadler and G. Nimtz, Phys. Rev. Lett. **56**, 382 (1986); G. Nimtz and J. Gebhardt, in *Proceedings of the 18th International Conference on the Physics of Semiconductors,* edited by O. Engström (World Scientific, Singapore, 1987), p. 1197.

[17]T. F. Rosenbaum, S. B. Field, D. A. Nelson, and P. B. Littlewood, Phys. Rev. Lett. **54**, 241 (1985); S. B. Field, D. H. Reich, B. S. Shivram, T. F. Rosenbaum, D. A. Nelson, and P. B. Littlewood, Phys. Rev. B **33**, 5082 (1986).

[18]M. Shayegan, H. D. Drew, D. A. Nelson, and P. M. Tedrow, Phys. Rev. B **31**, 6123 (1985).

[19]M. Shayegan, V. J. Goldman, H. D. Drew, D. A. Nelson, and P. M. Tedrow, Phys. Rev. B **32**, 6952 (1985).

[20]M. Shayegan, V. J. Goldman, H. D. Drew, N. A. Fortune, and J. S. Brooks, Solid State Commun. **60**, 817 (1986).

[21]V. J. Goldman, H. D. Drew, M. Shayegan, and D. A. Nelson, Phys. Rev. Lett. **56**, 968 (1986).

[22]V. J. Goldman, M. Shayegan, and H. D. Drew, Phys. Rev. Lett. **57**, 1056 (1986).

[23]M. Shayegan, V. J. Goldman, and H. D. Drew, in *Proceedings of the 18th International Conference on the Physics of Semiconductors,* Ref. 16, p. 1205.

[24]J. B. Choi, L. S. Kim, H. D. Drew, and D. A. Nelson, Solid State Commun. **65**, 547 (1988).

[25]See, e.g., N. F. Mott and E. A. Davis, *Electronic Properties of Non-Crystalline Materials,* 2nd ed. (Clarendon, Oxford, 1979).

[26]*Localization, Interaction, and Transport Phenomena,* edited by B. Kramer, G. Bergman, and Y. Bruynseraede (Springer-Verlag, Berlin, 1985).

[27]N. F. Mott, J. Phys. (Paris) Colloq. **37**, C4-303 (1976); P. W. Anderson, *ibid.* **37**, C4-340 (1976); D. J. Thouless, *ibid.* **37**, C4-349 (1976).

[28]B. I. Shklovskii and A. L. Efros, *Electronic Properties of Doped Semiconductors* (Springer-Verlag, New York, 1984). We limit ourselves here to the most frequently experimentally encountered situation of moderate compensation K, as opposed to the cases $K \ll 1$ or $1-K \ll 1$, when ionized impurity potential fluctuations on the length scale of $(Kn)^{-1/3}$ or $[(1-K)n]^{-1/3}$, respectively, play an important role.

[29]D. Romero, M.-W. Lee, H. D. Drew, M. Shayegan, and B. S. Elman, in *Anderson Localization (Springer Proceedings in Physics),* edited by T. Ando and H. Fukuyama (Springer-Verlag, Berlin, 1988), p. 53; M.-W. Lee, D. Romero, H. D. Drew, M. Shayegan, and B. S. Elman, Solid State Commun. **66**, 23 (1988).

[30]V. J. Goldman and H. D. Drew, Phys. Rev. B **32**, 5543 (1985).

[31]D. A. Nelson, W. M. Higgins, R. A. Lancaster, R. P. Murosako, and R. G. Roy (unpublished).

[32]J. J. Dubowski, T. Dietl, W. Szymanska, and R. R. Galazka, J. Phys. Chem. Solids **42**, 351 (1981).

[33]J. B. Mullin and A. Royle, J. Phys. D **17**, L69 (1984).

[34]W. Zhao, C. Mazuré, F. Koch, J. Ziegler, and H. Maier, Surf. Sci. **142**, 400 (1984).

[35]O. G. Balev, P. I. Baranskii, G. V. Beketov, R. M. Vinetskii,

and O. P. Gorodnichii, Fiz. Tekh. Poluprovodn. **21**, 1021 (1987) [Sov. Phys.—Semicond. **21**, 625 (1987)].

[36]D. E. Aspnes and H. Arwin, J. Vac. Sci. Technol. A **2**, 1309 (1984).

[37]R. Dornhaus and G. Nimtz, in *Narrow Gap Semiconductors,* Vol. 98 of *Springer Tracts in Modern Physics,* edited by G. Höhler (Springer-Verlag, Berlin, 1983), p. 119.

[38]K. I. Amirkhanov and R. I. Bashirov, Fiz. Tverd. Tela (Leningrad) **8**, 2189 (1966) [Sov. Phys.—Solid State **8**, 1739 (1967)]; L. E. Gurevich and A. L. Efros, Zh. Eksp. Teor. Fiz. **43**, 561 (1962) [Sov. Phys.—JETP **16**, 402 (1963)].

[39]K. Suizu and S. Narita, quoted in Fig. 75 of Ref. 37.

[40]R. Dornhaus, G. Nimtz, W. Schlabitz, and H. Burkhard, Solid State Commun. **17**, 837 (1975).

[41]B. I. Shklovskii, Fiz. Tekh. Poluprovodn. **6**, 1197 (1972) [Sov. Phys—Semicond. **6**, 1053 (1973)]; see also Ref. 28, Chap. 7.

[42]M. Pepper, J. Non-Cryst. Solids **32**, 161 (1979).

[43]For instance, in Figs. 13 and 14 as well as Figs. 7 and 8 we note that a linear dependence of ρ_{xy} on B above the *M-I* transition is observed only in a very limited field range. In fact, the InSb data show that, above $B_{M\text{-}I}$, ρ_{xy} (as well as ρ_{zz} and ρ_{xx}) has a much stronger than linear dependence on B (see, e.g., Fig. 1). The $Hg_{1-x}Cd_xTe$ data, on the other hand, indicate that ρ_{xy} (and ρ_{zz} and ρ_{xx}) has a much weaker dependence on B and its dependence even becomes sublinear at fields well above $B_{M\text{-}I}$ (due to the presence of the conducting surface layer).

[44]R. Mansfield, M. Abdul-Gader, and P. Fozooni, Solid State Electron. **28**, 109 (1985).

[45]S. Morita, N. Mikoshiba, Y. Koike, T. Fukase, S. Ishida, and M. Kitagawa, Solid State Electron. **28**, 113 (1985).

[46]P. A. Lee and T. V. Ramakrishnan, Rev. Mod. Phys. **57**, 287 (1985).

[47]Ishida and Otsuka (second paper in Ref. 3) reported $\delta=0.26$ for InSb. The discrepancy between their value and ours is likely to be due to the following factors. (1) The samples they studied had much higher compensation ($K>0.3$). (2) The densities of their samples were low so that the strong-field limit did not apply at the transition field. They therefore used variational parameters of Ref. 2 for $a_\perp^*$ and $a_\parallel^*$ instead of the strong-field-limit values used here. (3) Their definition of $B_{M\text{-}I}$ differs from ours.

[48]D. F. Holcomb and J. J. Rehr, Phys. Rev. **183**, 773 (1969).

[49]That is, it does not appreciably participate in the charge transport, although it may not be strictly localized according to P. W. Anderson, Phys. Rev. **109**, 1492 (1958) ((cf. V. G. Karpov, A. Ya. Shik, and B. I. Shklovskii, Fiz. Tekh. Poluprovodn. **16**, 1406 (1982) [Sov. Phys.—Semicond. **16**, 901 (1982)]).

[50]H. J. Juretchke, R. Landauer, and J. A. Swanson, J. Appl. Phys. **27**, 838 (1956).

[51]M. H. Cohen and J. Jortner, Phys. Rev. Lett. **30**, 696 (1973).

[52]Cf. R. E. Prange, Phys. Rev. B **23**, 4802 (1981).

[53]Both $a_\perp^*$ and $a_\parallel^*$ are smaller than the corresponding strong-field expressions $2l$ and $a^*/\ln\gamma$ (Refs. 2 and 41). At $\gamma=20$ the discrepancies are about 10% which leads to $a_\perp^2 a_\parallel$ smaller than $(a^*)^3/(\gamma\ln\gamma)$ by 30%, that is, a $\gamma=20$ data point is shifted by 30% to the left due to the use of the strong-field-limit approximation.

[54]M. Pollak and M. Ortuno, in *Electron-Electron Interactions in Disordered Systems,* edited by A. L. Efros and M. Pollak (Elsevier, Amsterdam, 1985).

[55]The factor h is greater than one and increases as the *M-I* transition is approached (Refs. 50 and 51).

[56]J. Gebhardt and G. Nimtz, Solid State Commun. **63**, 573 (1987).

[57]H. D. Drew, V. J. Goldman, and M. Shayegan, Solid State Commun. **63**, 575 (1987).

[58]Also, see G. Nimtz, J. Gebhardt, B. Schlicht, and J. P. Stadler, Phys. Rev. Lett. **55**, 443 (1985).

[59]See, e.g., G. Bauer, in *Solid State Physics,* Vol. 74 of *Springer Tracts in Modern Physics,* edited by G. Höhler (Springer-Verlag, Berlin, 1974), p. 1.

[60]M. Shayegan, V. J. Goldman, and H. D. Drew, Phys. Rev. Lett. **58**, 428 (1987).

[61]J. P. Maneval, A. Zylbersztejn, and H. F. Budd, Phys. Rev. Lett. **23**, 848 (1969).

[62]A. P. Long and M. Pepper, Physica (Amsterdam) **117&118B**, 75 (1983).

[63]G. Nimtz and J. P. Stadler, Phys. Rev. B **31**, 5477 (1985).

[64]B. A. Aronzon, A. V. Kopylov, and E. Z. Meilikhov, Fiz. Tekh. Poluprovodn. **21**, 1112 (1987) [Sov. Phys.—Semicond. **21**, 678 (1987)].

[65]W. S. Boyle and A. D. Brailsford, Phys. Rev. **107**, 903 (1957).

[66]R. F. Wallis and H. J. Bowlden, J. Phys. Chem. Solids **7**, 78 (1958).

[67]D. M. Larsen, J. Phys. Chem. Solids **29**, 271 (1968).

[68]Samples *Ha* and *Hb* were cut from the same wafer; the difference in the positions of CCR yields composition variation $\delta x=(dx/dm^*)_{x=0.2}\delta m^*\simeq 1\times 10^{-3}$.

[69]There is additional absorption in the low-field tail, probably (see second paper in Ref. 5) due to the photoionization transition $(000)\rightarrow(1^+)$.

[70]R. Bowers and Y. Yafet, Phys. Rev. **115**, 1165 (1959).

[71]We use donor level notation of H. Hasegawa and R. E. Howard, J. Phys. Chem. Solids **21**, 179 (1961).

[72]R. Kaplan, R. A. Cooke, R. A. Stradling, and F. Kuchar, in *The Application of High Magnetic Fields in Semiconductor Physics,* edited by J. F. Ryan (Clarendon, Oxford, 1978), p. 397.

[73]J. Perez, J. E. Furneau, and R. J. Wagner, J. Vac. Sci. Technol. A **6**, 2681 (1988).